Institution of Civil Engineers

ICE Research and Development Enabling Fund Grant 1021

Funders' Report

Surface settlements due to deep tunnels in clay

B D Jones MEng EngD CEng MICE

C R I Clayton BSc MSc DIC PhD CEng FICE CGeol FGS

Document No: 1021 03

8th October 2012

Issue and Approval Control Sheet

Client:	ICE Research and Development Enabling Fund
Address:	Institution of Civil Engineers, One Great George Street, Westminster, London, SW1P 3AA
Project:	1021 – Surface settlements due to deep tunnels in clay
Document Title:	Funders' Report – Surface settlements due to deep tunnels in clay
Document No:	1021 03

Issue	Version No.	Date	Format
For Comment	01	20th July 2012	pdf
Issue to C. Paulsen for comment	02	28th July 2012	pdf
Issue to J. Powell for comment	03	8th October 2012	pdf

	Name	Signature and Date
Prepared by:	Benoît Jones, University of Warwick	
Checked by:	Chris Clayton, University of Southampton	
Approved by:	John Powell on behalf of the ICE R&D Enabling Fund	

CONTENTS

CONTENTS

FOREWORD

This funders' report is the outcome of research grant no.1021, "Surface and subsurface settlements due to tunnelling" provided by the ICE Research and Development Enabling Fund. It has been written by Dr B D Jones of the University of Warwick (formerly of Morgan Sindall plc at the time of grant application) and Professor C R I Clayton of the University of Southampton.

ACKNOWLEDGEMENTS

The Honor Oak to Brixton case history presented in this report was based on data provided by Morgan Sindall, with the permission of the client, Thames Water. Answers to many queries were provided by the site team; in particular Carl Bradley, Anne Buttler, David Brown and Alastair Cruickshank. Colin Eddie and Kate Cooksey of Morgan Sindall Underground Professional Services also provided information on design and geology and support for the funding application.

The ICE R&D Enabling Fund Reviewer for this project was ICE R&D Enabling Fund Trustee John Powell.

The authors gratefully acknowledge the financial assistance of the ICE R&D Enabling Fund and the assistance provided by their respective employers.

1 INTRODUCTION

As the underground space in our urban centres becomes increasingly congested, linear tunnels are being constructed ever deeper to avoid existing underground infrastructure. Although deeper tunnels generally present less risk of excessive settlement at the surface, it is still necessary to attempt to predict those settlements, and to predict the larger settlements that may be experienced by underground structures much closer to the tunnel horizon.

Predictions of ground movements due to tunnelling rely heavily on empirical methods, which are based on published case studies of tunnels constructed in similar ground conditions. Until Jones (2010) published a case study of the Stoke Newington to New River Head tunnel, constructed at depths of 40 – 60m, no case studies existed of tunnels constructed below 35m. In this report, a 'deep' tunnel is defined as one that is deeper than 35m.

The Stoke Newington to New River Head data showed that established relationships between trough width and the depth of the tunnel significantly overpredicted the width of the settlement trough. This was corroborated by the subsurface movements measured in the Northern Line Tunnels and the HS1 tunnels. A new relationship between trough width parameter and height above the tunnel was proposed which fit well not just to the Stoke Newington to New River Head surface and subsurface settlement data, but also fit well to the many published case histories of surface and subsurface settlements at heights above the tunnel of less than 35m.

Although the evidence appeared to support the conclusions, they were expressed tentatively. On the one hand this was because all the data came from a single tunnel, and more data from more tunnels would increase confidence, and on the other hand the reliability of the Gaussian curve-fitting procedure was not known when the measurement error due to background movements was of the same order of magnitude as the settlements induced by tunnelling.

In order to address these issues, Chapter 2 focusses on the reliability of Gaussian curve-fitting, which is tested by running Monte Carlo analyses with fictional datasets. Next Chapter 3 presents new measurements of trough widths from the Honor Oak to Brixton tunnel at depths between 34 and 42m. Chapter 4 reinterprets the Stoke Newington to New River Head data in the light of the findings from the Monte Carlo analyses. This is then followed by a discussion in Chapter 5 and conclusions in Chapter 6.

2 SETTLEMENT MONITORING AND CURVE-FITTING FOR LOW VOLUME LOSS TUNNELS

The pattern of surface settlement induced transverse to a tunnel under construction may be described by a 'Gaussian' settlement trough, which is an inverted normal distribution curve.

Fitting a Gaussian curve to real settlement data is of practical use because the parameters that describe the curve; namely volume loss, maximum settlement and trough width, are conceptually easy to understand and can be compared at different locations and for different tunnel sizes, depths and construction methods.

For relatively low-risk tunnels, where predicted settlements are small, the level of risk will not usually merit the use of sophisticated surveying methods and the disruption at the surface they may

cause. In these cases, the industry best practice method of monitoring surface settlements is to use a precise laser level and bar-coded invar staff to level a transverse array of monitoring points, consisting of road nails inserted into the pavement or road surface. Where possible surfacing types such as paving slabs that may be unstable are avoided in favour of more solid objects such as kerb stones. Although some monitoring points do experience instability, if sufficient background readings are taken these points can be easily identified and removed from the dataset. The repeatability of this surveying method based on background readings has been found to be better than ±0.5mm (Jones, 2010).

Where this surface settlement monitoring method is used, and the magnitude of surface settlements is small, it can be difficult to obtain the Gaussian curve parameters because the magnitude of the potential measurement error is of the same order as the magnitude of the surface settlements themselves. Guidance is required on the best objective method of curve-fitting, and what confidence one can have in the derived Gaussian curve parameters for a given arrangement of monitoring points and a given magnitude of settlement.

Four different methods of fitting Gaussian curves to real data will be compared for different array types, settlement magnitudes and trough widths with the aim of providing guidance on confidence limits for Gaussian curve parameters back-calculated from real data.

2.1 Settlement trough geometry

Surface and subsurface ground settlements due to tunnelling are commonly characterised by a 'Gaussian' curve attributed to Peck (1969) and Schmidt (1969), which takes the form of an inverted normal (or Gaussian) distribution curve transverse to the direction of the tunnel drive. This is illustrated in Figure 1.

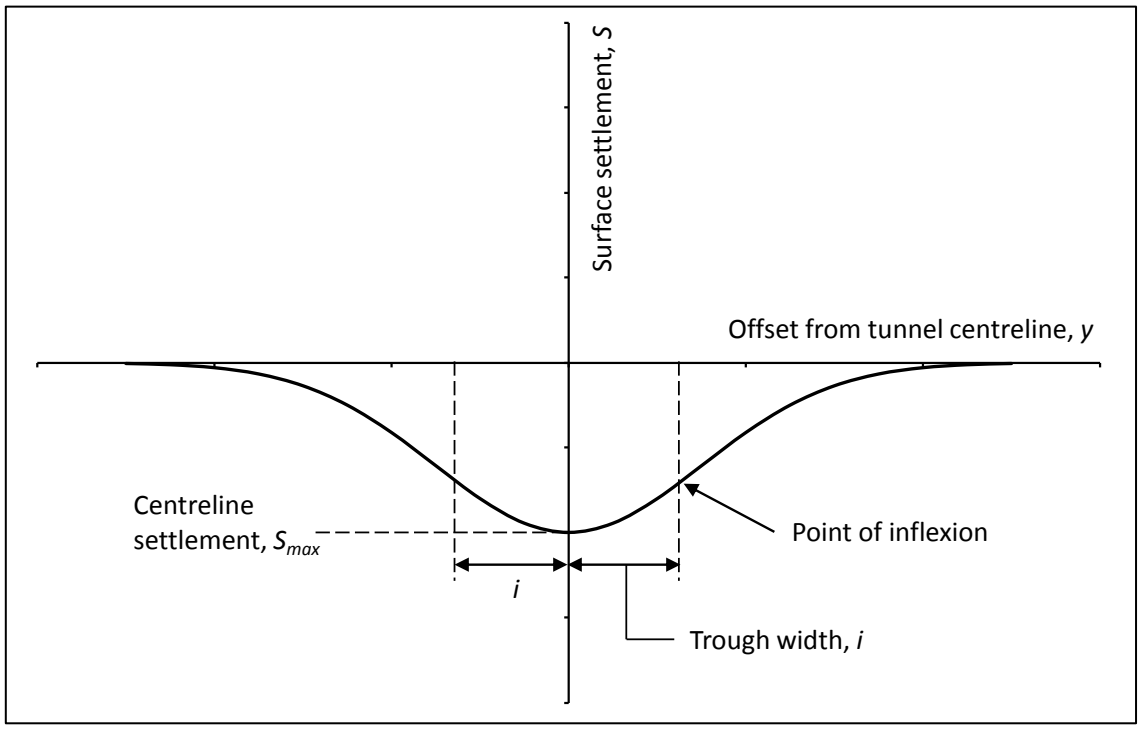

Figure 1: Gaussian settlement trough

The distance from the centreline to the point of inflexion of the curve, which in a normal distribution would be the standard deviation, is known as the 'trough width', *i*. The maximum settlement over the centreline of the tunnel S_{max} is analogous to the mean of a normal distribution. Settlement *S* at offset *y* from the tunnel centreline is therefore given by:

$$S = S_{\max} \exp\left(-y^2/2i^2\right) \qquad \text{(Equation 1)}$$

The area under the curve is defined as the 'volume loss', V_s. This may be given by the following equation:

$$V_s = \int_{-\infty}^{\infty} S\,dy = \int_{-\infty}^{\infty} S_{\max} \exp\left(-y^2/2i^2\right)dy = \sqrt{2\pi}\, i\, S_{\max} \qquad \text{(Equation 2)}$$

Using Equations 1 and 2 or combinations thereof, the curve may be defined by any two of the parameters V_s, S_{max} or *i*.

The trough width may be estimated by multiplying the height above the tunnel by the 'trough width parameter', *K*, which is estimated by consideration of case histories. Trough width parameter, *K*, is related to trough width, *i*, by the following equation:

$$i = K\left(z_0 - z\right) \qquad \text{(Equation 3)}$$

where z_o is the depth to axis of the tunnel under construction, and *z* is the depth to the point under consideration, where $z \le z_o$. At the surface, $z = 0$.

The Gaussian curve is a useful tool, as it allows comparison of settlements at different locations and on different projects by a small number of practically relevant parameters. This then facilitates the empirical prediction of the magnitude of settlement (as described by volume loss V_s or maximum settlement S_{max}) and its extent (described by trough width *i*). Empirical prediction is usually based on a meta-analysis of case histories. This meta-analysis may be refined by restricting the list of case histories considered to consist of, for example, only those tunnels using the same excavation and support method at similar depth and with similar geology, or by using correlations that take some or all of these factors into account.

2.2 Methods of Gaussian curve-fitting to real settlement monitoring data

To plot a Gaussian curve, at least two parameters must be known, which can be any two of V_s, S_{max} or *i*. Therefore, curve-fitting is not straightforward as there are two variables.

The actual methods used to fit a Gaussian curve to real data are seldom described in the literature. Only New & Bowers (1994) mention the use of nonlinear regression analysis to calculate Gaussian curve parameters. Nowhere, except in Jones (2010), are the methods used actually described in any detail.

There are at least 5 possible methods of curve-fitting:

1. **DCJ** - Direct calculation of volume loss, V_s, by trapezoidal integration of the settlement monitoring data, followed by a direct calculation of trough width, *i* by exploiting the analogy to the error function standard deviation (this is the method used in Jones, 2010).
2. **DCSMAX** - Direct calculation of volume loss, V_s, by trapezoidal integration of the settlement monitoring data, followed by a direct calculation of trough width , *i* , for each of the data

points not on the centreline, by assuming that the measured S_{max} value is correct. These values of trough width i are then averaged.

3. **NRSAE** - Use of nonlinear regression, varying both V_s and i to find the minimum sum of absolute errors (SAE). Here 'error' is defined as the difference between the measured monitoring data value and the Gaussian curve value at the same offset, also known as a 'residual' in regression analysis.
4. **NRLS** - Use of nonlinear regression, varying both V_s and i, this time to find the minimum value of the sum of the residuals squared. This is known as the 'nonlinear least squares' method in regression analysis.
5. **By eye** – Varying volume loss, V_s, and trough width , i , until the curve appears to visually fit the data.

The direct methods, DCJ and DCSMAX, have the advantage that a single calculation, i.e. in one cell of a spreadsheet, is required for each data set (one set of readings from one settlement monitoring array). For the nonlinear regression methods, NRSAE and NRLS, a large table of values must be used in a spreadsheet, or a bespoke computer program may be used.

Fitting a Gaussian settlement trough 'by eye' is subjective. Often a subconscious assumption will be made, for instance, that the curve must pass through the maximum settlement, or that the trough width is assumed to be equal to an empirical prediction. This method will not be discussed further.

It is not possible to compare the goodness of fit of these methods by applying them to real data, since they each use a different criterion for goodness of fit. However, a comparison may be made by using each of these methods in a Monte Carlo analysis with a large number of fictitious monitoring data sets.

Each fictitious data set begins with the same 'perfectly Gaussian' set of data at fixed offsets from the centreline, with a predetermined volume loss and trough width. Then each data point is assigned a random error. This is a Monte Carlo analysis (rather than a 'What if?' analysis), in that the assigned random errors follow a normal distribution. Therefore, the mean values of volume loss and trough width should approach the original 'perfectly Gaussian' values after a sufficiently large number of randomised data sets have been used. Once convergence has been achieved, the geometric mean and geometric standard deviation of trough width i and the mean and standard deviation of trough volume V_s will provide a means of comparing the accuracy of the curve-fitting methods.

Each of the curve-fitting methods are described in more detail in the following sub-sections.

2.2.1 DCJ method

When a Gaussian curve is used to represent ground movements due to tunnelling, by analogy the standard deviation or the point of inflexion is the trough width, i, and the frequencies are the settlements, S. Therefore, the trough width may be calculated directly from the data by calculating the standard deviation about a mean assumed to be at the centreline of the tunnel. The volume loss is also required to define the curve and this was calculated by trapezoidal integration of the settlements over the extent of the array and correcting for any missing tails.

The standard deviation σ, or the trough width i, is given by:

$$\sigma = \sqrt{\frac{\sum_{j=1}^{n}[y_j^2 S_j]}{\sum_{j=1}^{n}[S_j]}} = i \qquad \text{(Equation 4)}$$

where j is the point number from 1 to n,

n is the number of points in an array,

y_j is the transverse distance of point j from the tunnel centreline,

and S_j is the measured settlement of point j.

This equation is sensitive to errors at large offsets, so judgement should be exercised to exclude errors at large offsets where the settlement should be negligible. The equation will also be less accurate when the spacing of monitoring points is not constant, since it is a standard equation for a histogram of frequencies.

Note that Equation 4 is slightly different to Equation 1 in Jones (2010). This is because the equation for the 'population standard deviation' should have been used rather than the 'sample standard deviation', which includes a '-1' term in the denominator.[1]

The measured volume loss using trapezoidal integration, V_{lm}, is given by:

$$V_{lm} = \frac{\sum_{j=1}^{n-1}\left[\left(\frac{S_j + S_{j+1}}{2}\right)(y_j - y_{j+1})\right]}{A_f} \qquad \text{(Equation 5)}$$

where A_f is the excavated face area of the tunnel.

The numerator of the quotient in Equation 5 is basically a trapezoidal integration of the settlement data. If the data doesn't cover the whole of the settlement trough, for example because the trough width was larger than expected or because points could not be installed due to the presence of buildings or other obstructions, the actual volume loss, V_s, may be estimated by using the following equation:

$$V_l = \frac{V_{lm}}{\int_{-\infty}^{x_n} \frac{1}{\sqrt{2\pi}\sigma} e^{-\left(\frac{y^2}{2\sigma^2}\right)} - \int_{-\infty}^{x_1} \frac{1}{\sqrt{2\pi}\sigma} e^{-\left(\frac{y^2}{2\sigma^2}\right)}} \qquad \text{(Equation 6)}$$

where the two terms in the denominator represent the unit cumulative distribution from minus infinity to x_1 and x_n, i.e. the denominator is the proportion of the total volume loss that is within the limits of the array.

Trapezoidal integration is reasonably accurate, since the missing volumes due to curvature between data points in the hogging and sagging parts of the curve to an extent cancel each other out. The accuracy depends on the spacing of the monitoring points and their locations relative to the trough width.

[1] In Chapter 4, the Stoke Newington to New River Head tunnel Gaussian curve parameters have been corrected to account for this. The values did not change significantly and do not alter the conclusions of that paper.

2.2.2 DCSMAX method

This method uses a trapezoidal integration to calculate volume loss, in the exactly the same manner as for the DCJ method.

The trough width, *i*, is calculated for each value of settlement S_j by reformulating Equation 1 as follows:

$$i = \sqrt{\frac{-y^2}{2.\ln(S_j/S_{max})}} \qquad \text{(Equation 7)}$$

The assumption is made that the centreline settlement, S_{max}, is correct. Since it is usually the largest settlement in an array, measurement error is likely to have less effect, proportionally. Trough width, *i*, is calculated for each point in the array (except the centreline point), and the values averaged.

2.2.3 NRSAE method

When implemented in a spreadsheet, this method creates a large table with volume loss incrementally varying in each row, and trough width incrementally varying in each column. A simplified example is shown in Table 1.

In each cell, the sum of the absolute errors (SAE) is calculated for the corresponding values of volume loss and trough width. The sum of the absolute errors is the sum of the absolute values of the differences between the calculated Gaussian curve values of settlement and the monitoring data settlements at each offset. The minimum value of SAE is then found by searching the table and the corresponding values of volume loss and trough width describe the best fit Gaussian curve.

In order to have a manageable size of table, initially the values of volume loss and trough width used in the table were given a large range and large increments between cells. The range and hence the resolution were then decreased iteratively, focussing the range onto the best fit values. The final values were determined with a maximum resolution of 0.05m for trough width and 0.5% of the total area under the settlement trough for trough volume.

Trough volume (mm.m)		Trough width (m)				
		10.0	10.5	11.0	11.5	etc…
	0.3					
	0.4					
	0.5					
	etc…					

Table 1: Simplified example table for nonlinear regression method

In each cell of Table 1, the following equation was used to calculate SAE:

$$SAE = \sum_{j=1}^{n} \left| \frac{V_s}{\sqrt{2\pi}.i} exp\left(\frac{-y_j^2}{2i^2}\right) - S_j \right| \quad \text{(Equation 8)}$$

Where V_s and i vary from cell to cell, and S_j is data point j from a fictitious settlement array with n monitoring points. So in each cell a Gaussian curve is tried and the goodness of fit is output as the SAE value.

2.2.4 NRLS method

This method works in a similar manner to the NRSAE method, but in each cell of the table the differences between the calculated Gaussian curve values of settlement and the monitoring data settlements at each offset are squared and then added together. This is known as the 'least squares' value (LS). The minimum cell value in the table is then found and the corresponding values of volume loss and trough width describe the best fit Gaussian curve.

The equation used in each cell to calculate LS was:

$$LS = \sum_{j=1}^{n} \left(\frac{V_s}{\sqrt{2\pi}.i} exp\left(\frac{-y_j^2}{2i^2}\right) - S_j \right)^2 \quad \text{(Equation 8)}$$

The NRLS method may give different results to the NRSAE method, because more emphasis is placed on minimising larger errors because the errors are squared when calculating the LS value. However, in tests the NRLS method was found to give similar results to the NRSAE and so analysis of all the array types, trough widths and error ratios was not performed.

2.3 Factors under investigation

Factors affecting the goodness-of-fit of a Gaussian curve to the randomised data are:

1. The magnitude of the applied errors, relative to the magnitude of the settlements. This is described by the ratio S_{max}/σ_{mc} , where σ_{mc} is the standard deviation of the applied errors. This is a direct analogy to the repeatability of settlement monitoring in the field, assuming measurement errors are random and independent and follow a normal distribution. Note that some errors may not be independent, for instance movement of a benchmark, which will affect all the measured settlements in the array.
2. The spacing of the monitoring points in a transverse settlement monitoring array, both in terms of magnitude and uniformity of spacing (often settlement monitoring points are spaced further apart away from the centreline of the tunnel)
3. The trough width relative to the monitoring point spacing.

Therefore, these factors have been varied in the Monte Carlo analysis to follow.

2.3.1 Codes used in analyses

Codes have been used to simplify the presentation of the analyses. These consist of the array type, the trough width, then the centreline settlement, as shown in the following example:

A7.5-5 = Array type A, trough width 7.5m, centreline settlement 5mm.

2.3.2 Convergence criterion

A convergence criterion is required to demonstrate when sufficient randomised data sets have been used. At this point, further sampling will not change the values of the mean and standard deviation of trough width and volume loss that have been determined.

For trough width *i* this has been defined as when the instantaneous geometric mean and geometric standard deviation do not vary from the overall mean value by more than ± 0.1m over the last 50 data sets. The geometric mean and geometric standard deviation were used because the determined values of *i* follow a lognormal distribution. This is because *i* cannot be less than zero, but in rare cases it can be substantially larger than the expected value, particularly for low error ratios. Lognormal distributions occur when the natural logarithm of a variable follows a normal distribution. This follows from the form of Equation 1, since the settlements *S* follow a normal distribution and *S* is related to the exponential of *i*.

For trough volume V_s, convergence has been defined as when the instantaneous mean and standard deviation values of trough volume have not varied from the overall mean value by more than ± 1.0% of the expected mean value of trough volume over the last 50 data sets (e.g. for a theoretical 37.6mm.m trough volume, the mean and standard deviation must not vary by more than ± 0.376mm.m).

In addition, a minimum number of 100 randomised data sets were used.

For one array (A7.5-2), more datasets were sampled in order to better understand convergence and ensure that the criteria were valid. This is shown in Figure 2, Figure 3 and Figure 4 for the NRSAE method.

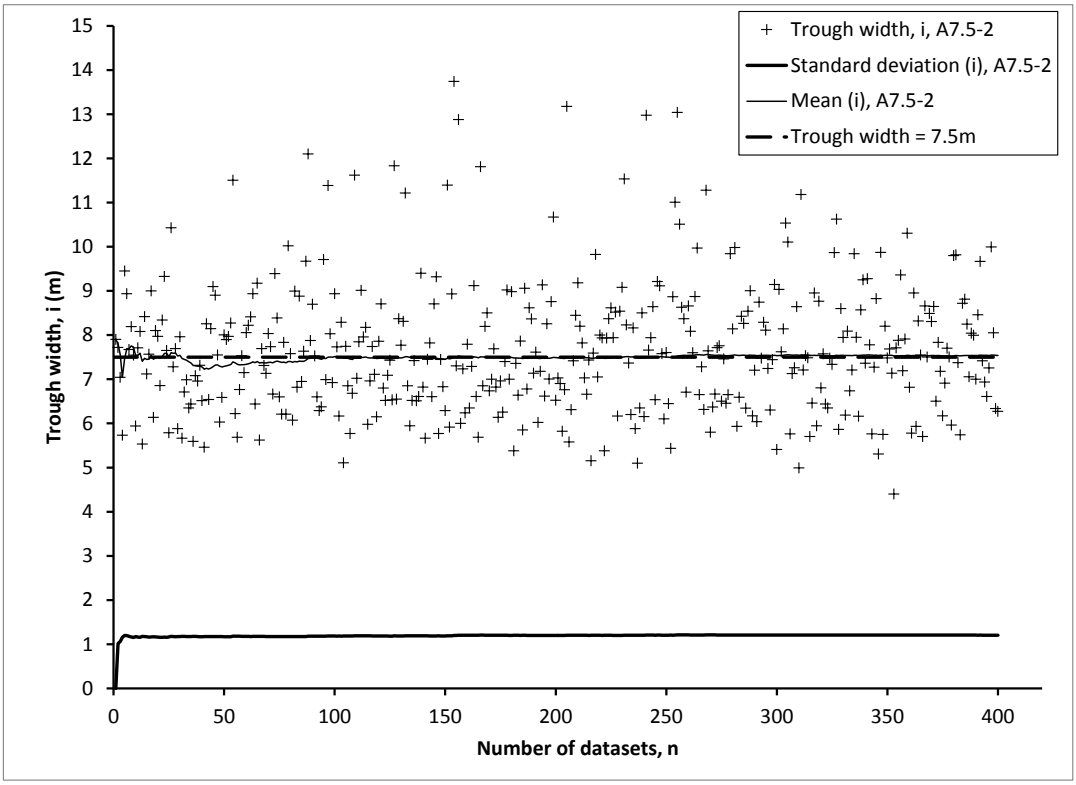

Figure 2: Mean and standard deviation of trough width vs. number of datasets (A7.5-2)

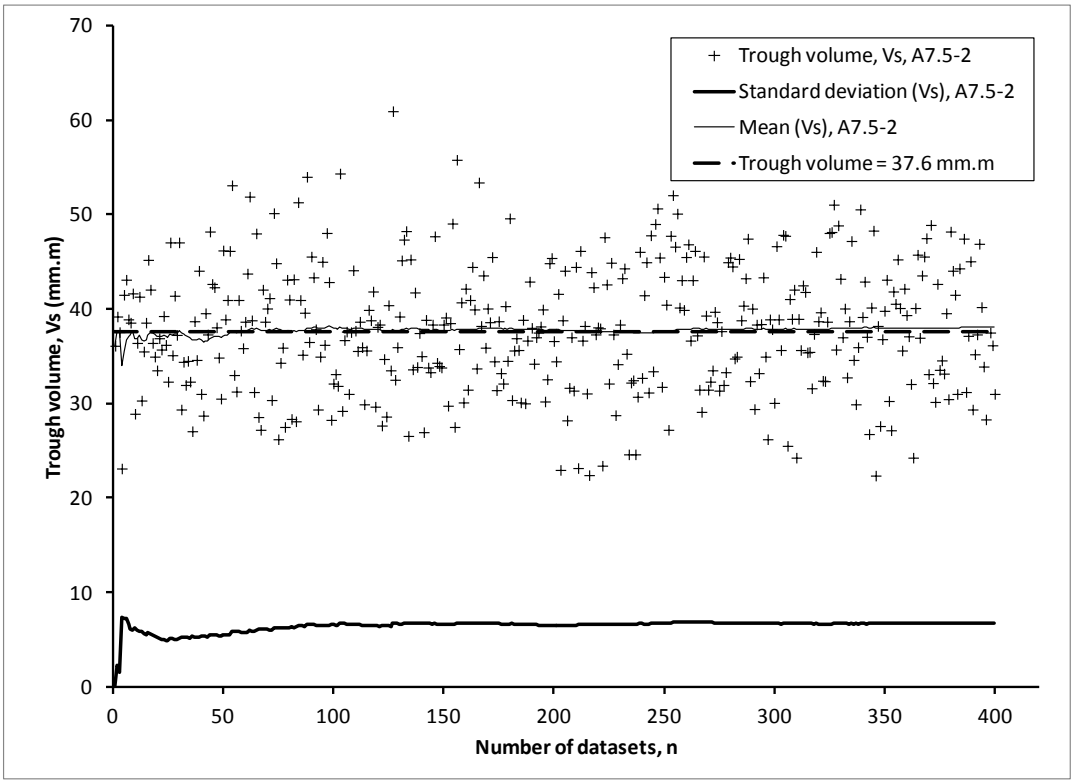

Figure 3: Mean and standard deviation of trough volume vs. number of datasets (A7.5-2)

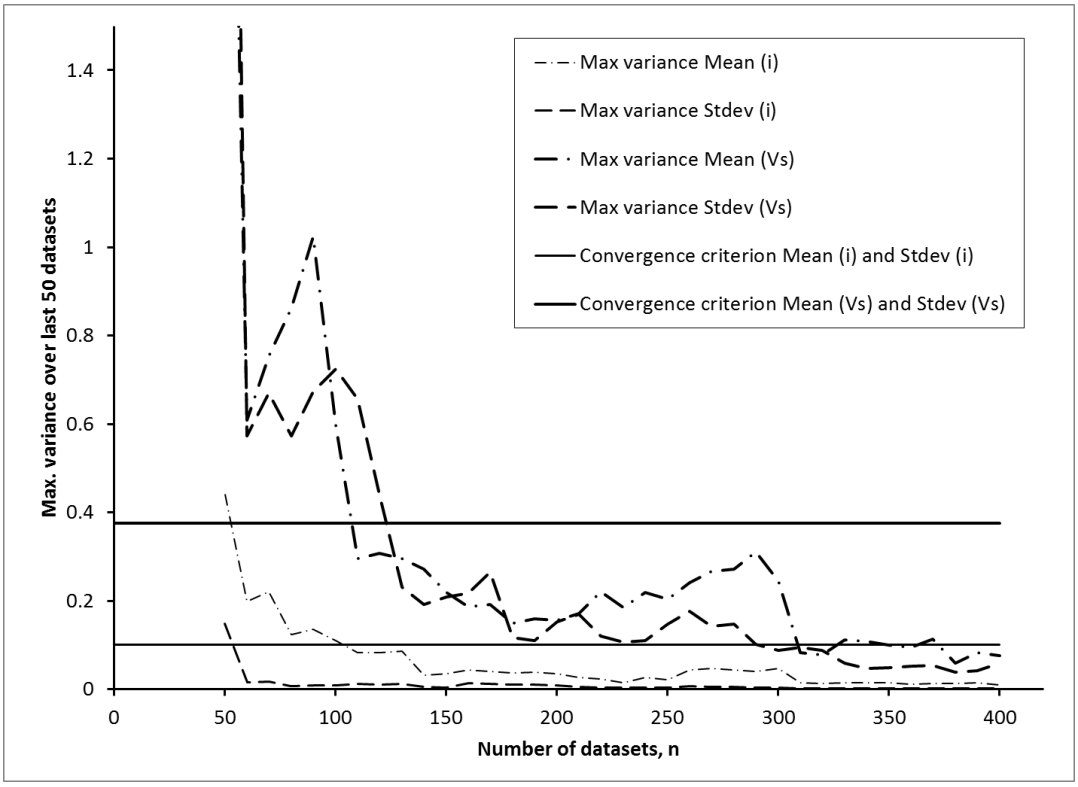

Figure 4: Monte Carlo analysis convergence criteria for mean and standard deviation of trough width and trough volume (A7.5-2)

Figure 2 and Figure 3 show that with increasing number of datasets, the mean and standard deviation curves become smoother as new outliers have less impact on an already large sample size.

Figure 4 shows the maximum variance of mean and standard deviation of trough width and trough volume over the last 50 datasets against the total number of datasets. As the total number of datasets increases, the maximum variance tends to decrease and the curves become smoother. This shows that if the convergence criteria are met, in this case after 140 datasets have been sampled, the mean and standard deviation are unlikely to exceed this value by a significant amount as volatility has been damped to a sufficient degree.

If the convergence criteria cannot be met, this will be noted in the graphs and tables showing the results and the maximum variance over the last 50 datasets value quoted.

2.3.3 Array types

Three types of transverse settlement arrays were used, denoted A, B and C. These are detailed in Table 2 below.

Array type	*n*	Offsets of points 1 to *n* (m)
A	5	-25, -10, 0, 10, 25
B	11	-35, -25, -15, -10, -5, 0, 5, 10, 15, 25, 35
C	21	-50, -45, -40, -35, -30, -25, -20, -15, -10, -5, 0, 5, 10, 15, 20, 25, 30, 35, 40, 45, 50

Table 2: Array types used in Monte Carlo analysis

Array type A represents a settlement monitoring array that could be used for low-risk tunnels, for example a small diameter EPB TBM at depths greater than 20m. Arrays similar to this were used for the Honor Oak to Brixton Thames Water Ring Main extension tunnel.

Array type B represents a more detailed array with a wider extent, which may be used if better quality information on the Gaussian curve parameters is required. Arrays similar to this were used for the Stoke Newington to New River Head Thames Water Ring Main extension tunnel, where volume losses and trough widths were required to estimate much more critical subsurface settlements induced in third party tunnels further along the route.

Array type C represents the type of array that has been used in the past for research purposes and has been included to show the effect of using the most detailed array that is reasonably practical using precise levelling. More detail and accuracy could be obtained using a string of electrolevels or tiltsensor beams, for example, but in most cases this is not feasible at the ground surface.

In all three cases, it has been assumed that benchmarks have been installed sufficiently far away from the tunnel's zone of influence and that the settlements measured are absolute values and not relative to the outermost points.

2.3.4 Trough widths

Three trough widths have been used; 7.5m, 12.5m and 20m. This range will cover the vast majority of tunnel depths in a variety of soil types.

2.3.5 Centreline (maximum) settlement

Seven different values of centreline (maximum) settlement S_{max} have been used; 0.5mm, 1mm, 2mm, 5mm, 10mm, 20mm and 50mm. This range will cover the vast majority of tunnel diameters and tunnel depths with the given range of trough width values.

2.4 Comparison of curve-fitting methods using Monte Carlo analysis

In order for the results of the Monte Carlo analysis to be more easily applicable, the ratio between the centreline settlement S_{max} and the standard deviation of the random errors applied to the data σ_{mc} has been used. This will be referred to as the 'error ratio'. In general, if S_{max} is much larger than σ_{mc}, the error ratio will be large and the reliability of curve fitting will be much better than for a small error ratio where the errors are approaching the value of S_{max}.

$$Error\ ratio = \frac{S_{max}}{\sigma_{mc}} \qquad \text{(Equation 9)}$$

Therefore, Gaussian curve parameters calculated from small values of settlements when simple surveying methods are used for surface settlement monitoring will be less reliable. The aim of the Monte Carlo analyses is to quantify this in terms of confidence limits for trough width and volume loss for a given S_{max} value and the standard deviation of measurement error.

Since a single value of standard deviation of the applied random errors has been used, equal to 0.25mm, the values of error ratio listed in Table 3 are obtained.

Centreline settlement, S_{max} (mm)	Error ratio S_{max}/σ_{mc}
0.5	2
1	4
2	8
5	20
10	40
20	80
50	200

Table 3: Error ratios used in Monte Carlo analyses

2.4.1 Array type A trough width estimates

Figure 5, Figure 6 and Figure 7 show the values of mean and standard deviation of trough width using the NRSAE, DCJ and DCSMAX methods for trough widths 7.5m, 12.5m and 20m respectively, plotted against error ratio.

As expected there is a trend for increasing reliability of the determination of Gaussian curve parameters as the error ratio increases, both in terms of the mean and the standard deviation of the predicted values over a large number of randomised data sets sufficient to achieve convergence to stable values.

Note that since the geometric standard deviation is being used, it approaches 1.0 as the standard deviation approaches zero. The geometric standard deviation used here is the exponential of the standard deviation of the natural logarithms of the values.

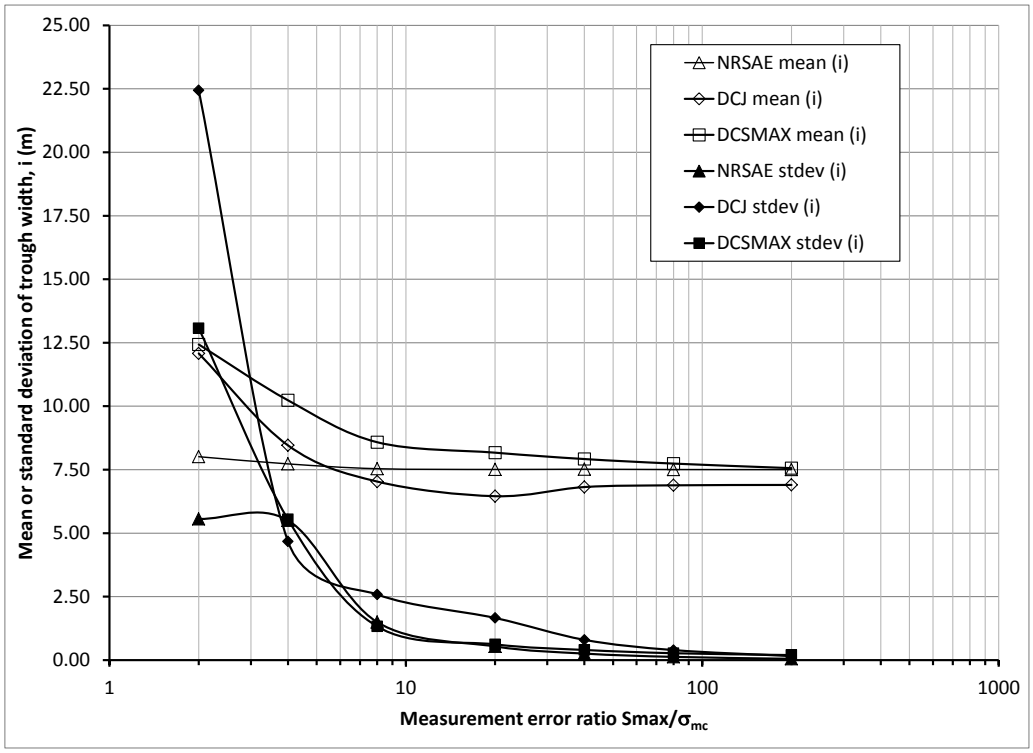

Figure 5: Variation of mean and standard deviation of Monte Carlo trough width values vs. error ratio for array type A, trough width 7.5m

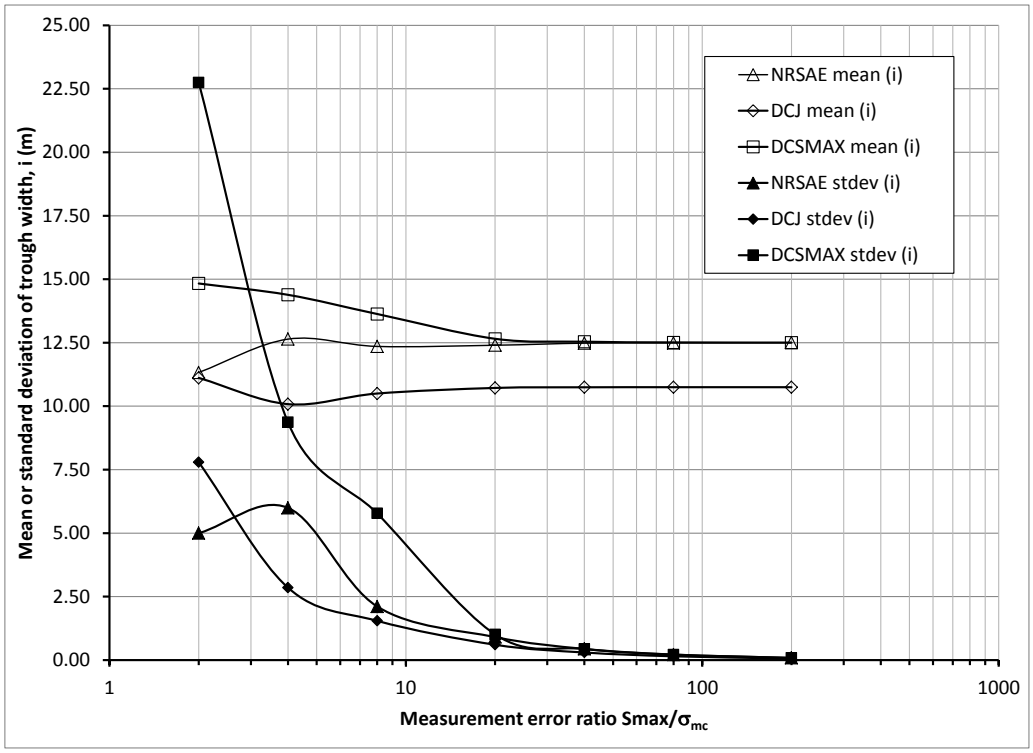

Figure 6: Variation of mean and standard deviation of Monte Carlo trough width values with error ratio for array type A, trough width 12.5m

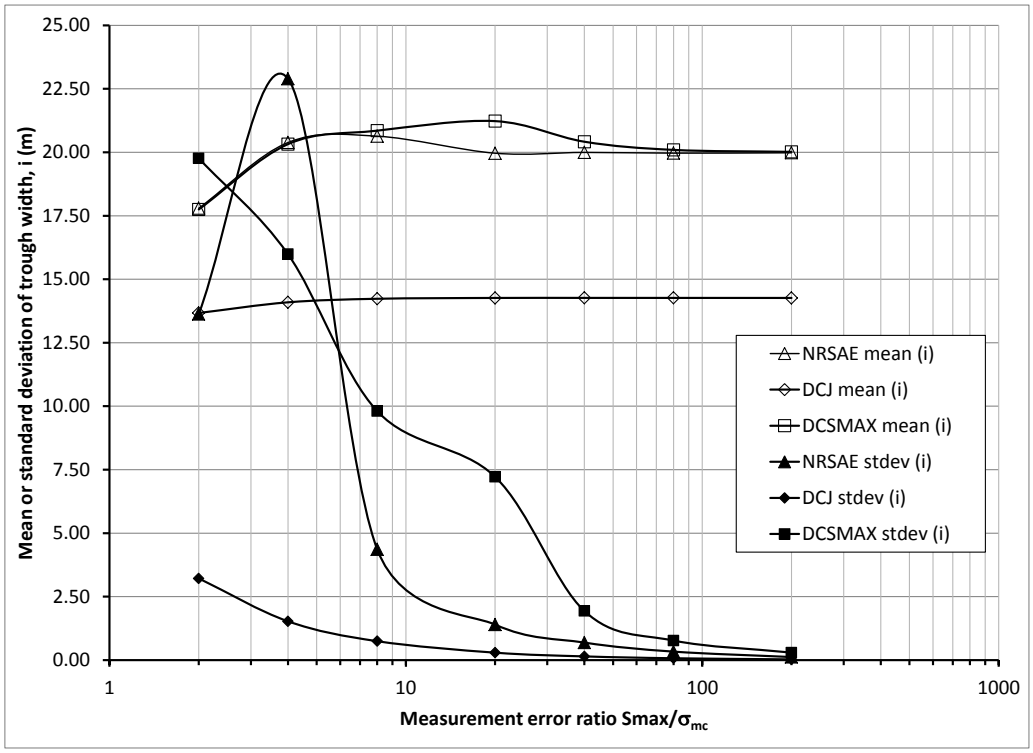

Figure 7: Variation of mean and standard deviation of Monte Carlo trough width values with error ratio for array type A, trough width 20m

2.4.2 Array type B trough width estimates

Figure 8 and Figure 9 show the values of mean and standard deviation of trough width using the NRSAE, DCJ and DCSMAX methods for trough widths 7.5m and 12.5m respectively, plotted against error ratio.

As expected there is a trend for increasing reliability of the determination of Gaussian curve parameters as the error ratio increases, both in terms of the mean and the standard deviation of the predicted values over a large number of randomised data sets.

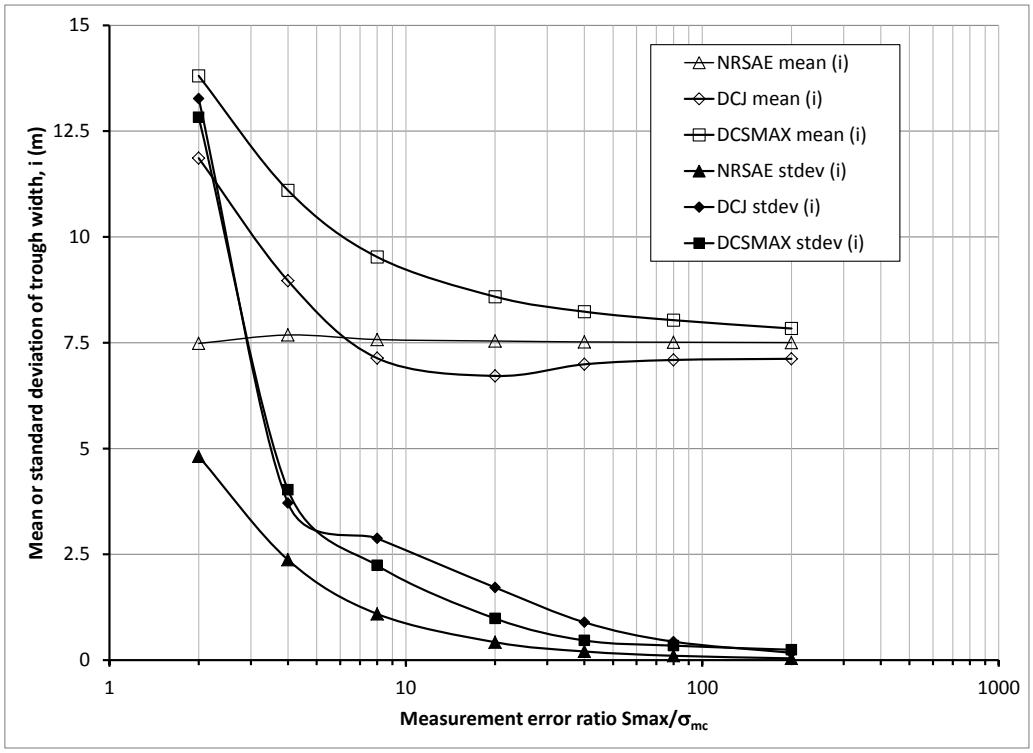

Figure 8: Variation of mean and standard deviation of Monte Carlo trough width values with error ratio for array type B, trough width 7.5m

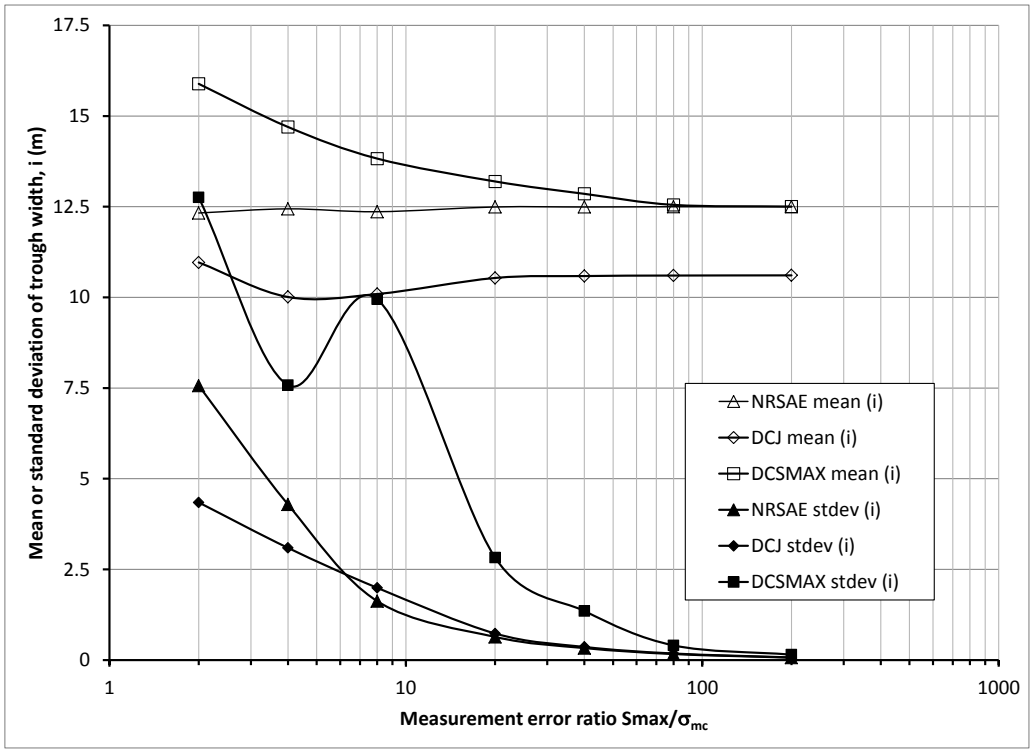

Figure 9: Variation of mean and standard deviation of Monte Carlo trough width values with error ratio for array type B, trough width 12.5m

2.4.3 Array type C trough width estimates

Figure 10 shows the values of mean and standard deviation of trough width using the NRAAE, DCJ and DCSMAX methods for a trough width of 12.5m, plotted against error ratio.

As expected there is a trend for increasing reliability of the determination of Gaussian curve parameters as the error ratio increases, both in terms of the mean and the standard deviation of the predicted values over a large number of randomised data sets.

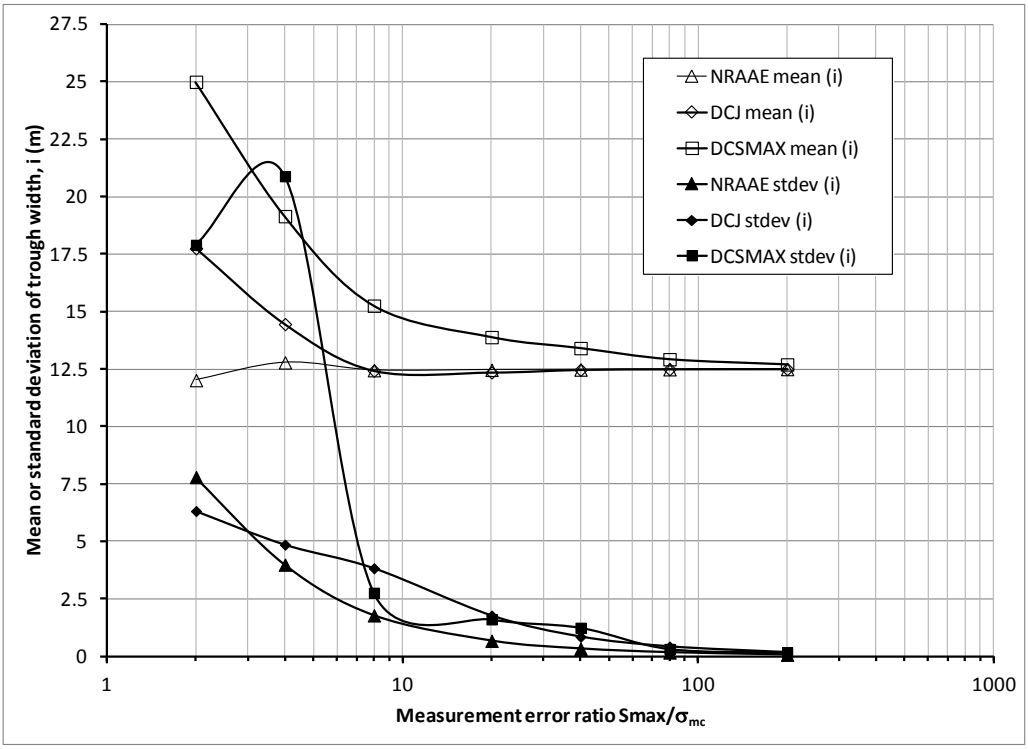

Figure 10: Variation of mean and standard deviation of Monte Carlo trough width values with error ratio for array type C, trough width 12.5m

2.4.4 Trough volume estimates

Back-calculations of trough volume were made either directly using a trapezoidal integration of the settlement data (the same method was used in both the DCJ and DCSMAX method, collectively described in this section as the 'DC' method), or in conjunction with a back-calculation of trough width using the NRSAE method.

For array type A, a comparison of the different trough volume calculation methods for the three values of trough width is shown in Figure 11. This shows that the DC method, over a large number of sampled data sets, is relatively insensitive to the error ratio, but does not converge on the correct trough volume. This is less pronounced for array type B and is a negligible effect for array type C. This is because the array does not cover the whole of the trough for array type A. Array type B has a large extent and array type C covers virtually all of the trough such that the errors are negligible. A correction for missing tails could be made, but this depends on the value of trough width *i*.

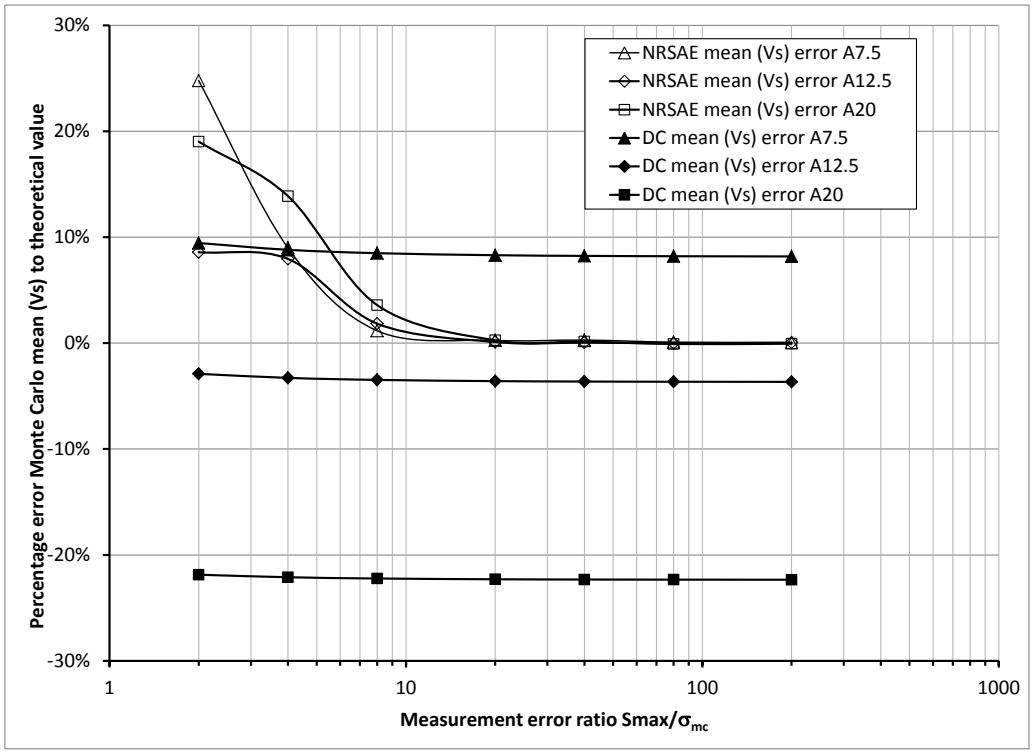

Figure 11: Percentage error of Monte Carlo mean with error ratio for DC and NRSAE methods of trough volume calculation, array type A, trough widths 7.5m, 12.5m and 20m

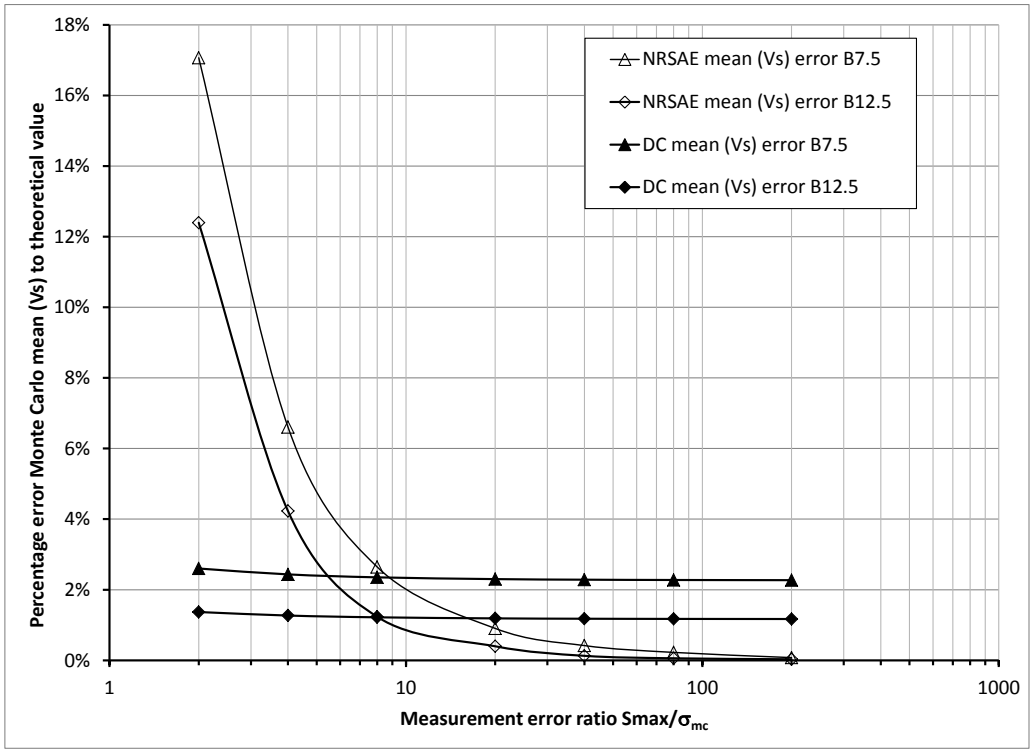

Figure 12: Variation of Monte Carlo mean with error ratio for DC and NRSAE methods of trough volume calculation, array type B, trough widths 7.5m and 12.5m

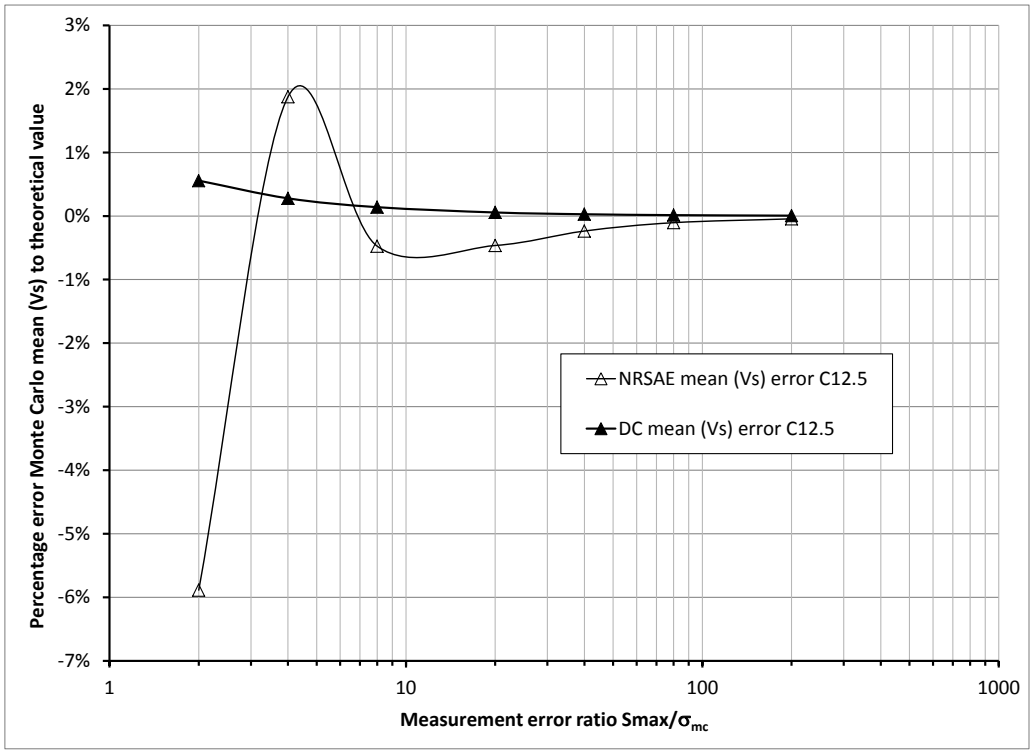

Figure 13: Percentage error of Monte Carlo mean with error ratio for DC and NRSAE methods of trough volume calculation, array type C, trough width 12.5m

In order to take account of the missing tails to verify that convergence to the correct value of trough volume would occur, without introducing errors from trough width calculation, the mean values determined by the Monte Carlo analysis can be compared to a trapezoidal integration of the perfect data before random errors are added. This is shown in Figure 14. It is perhaps unsurprising that the direct trapezdoidal integration converges to the ideal value in this case, since the settlement points have been given artificial random errors that follow a normal distribution and will cancel out if the population is large enough.

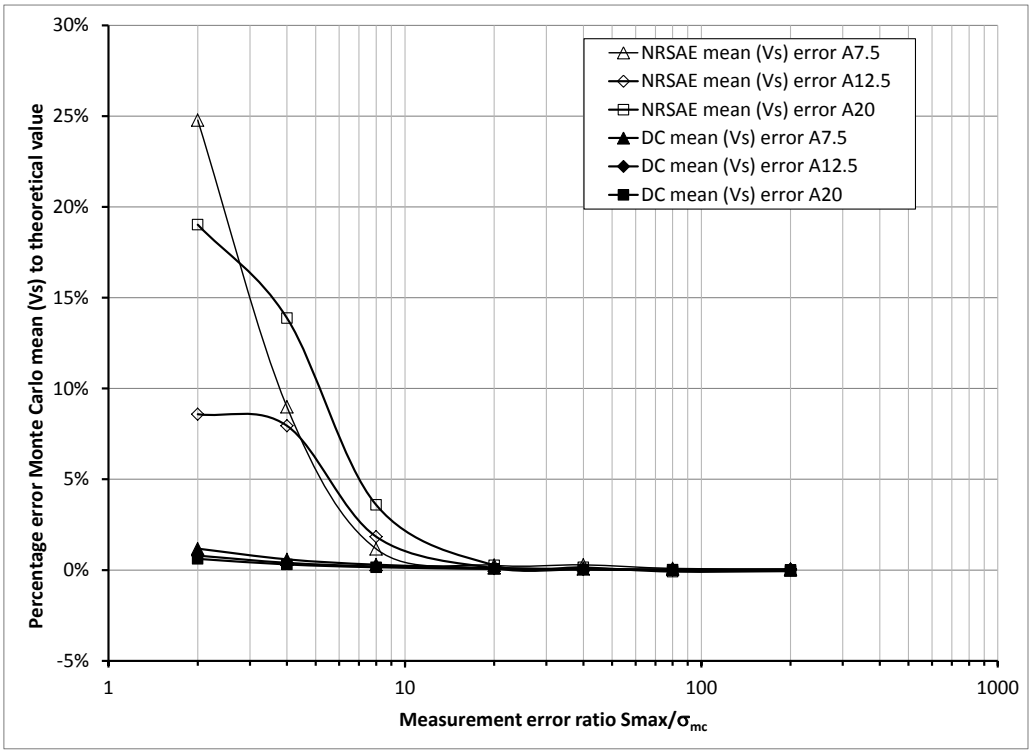

Figure 14: Percentage error of Monte Carlo mean with error ratio for DC and NRSAE methods of trough volume calculation, array type A, trough widths 7.5m, 12.5m and 20m

The real test of reliability is the standard deviation of trough volume. The standard deviation as a percentage of the theoretical trough volume is shown for array type A in Figure 15, array type B in Figure 16 and array type C in Figure 17. Here it can be seen that for all trough widths the standard deviation is smaller using the direct calculation as opposed to nonlinear regression. Another clear trend is that as the trough width increases the standard deviation of trough volume decreases.

There appears to be an anomaly in the NRSAE method at an error ratio of 4 (this is S_{max} = 1mm), which for a trough width of 20m means that the standard deviation is worse than for the error ratio of 2, which is unexpected. This was because it was not always possible to converge the nonlinear regression to a solution where the error ratio was small, as sometimes the errors conspired to make the curve very non-Gaussian. Therefore, for instance, the 'worst' 16 samples were left out of the A20-0.5 calculation of mean and standard deviation, but only 4 of these didn't converge in the A20-1 calculation and so were included. Since the same randomised values were used for the different error ratios, these 12 samples had a significant effect on the A20-1 standard deviation by contributing outliers to the population.

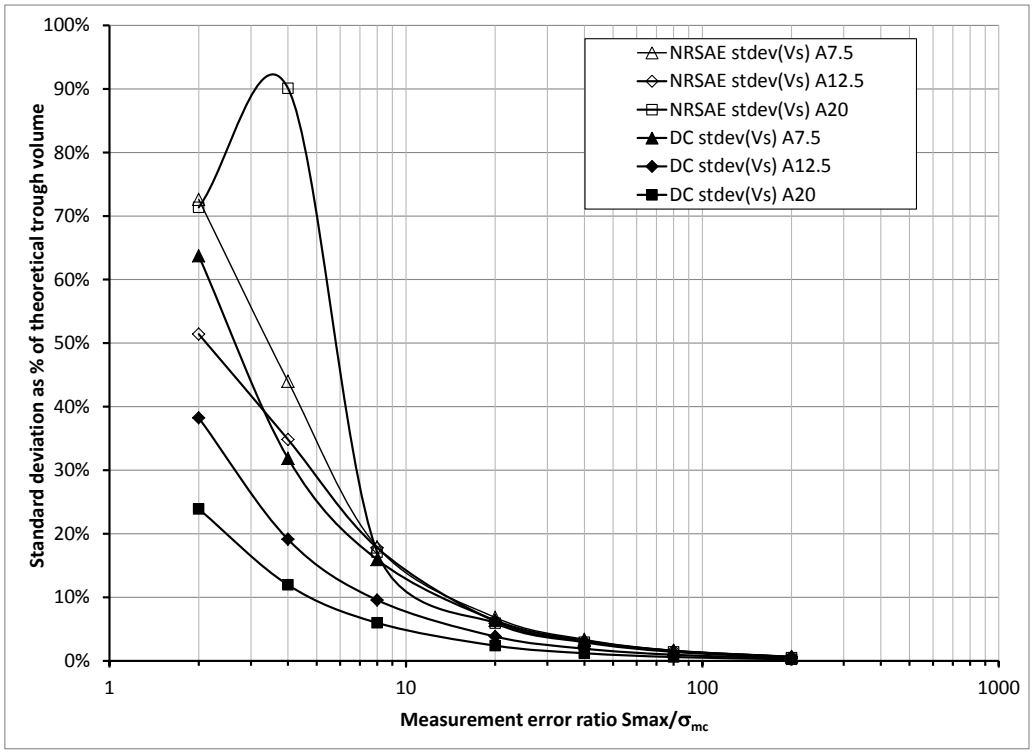

Figure 15: Monte Carlo standard deviation of trough volume as a percentage of theoretical trough volume for array type A, trough widths 7.5m, 12.5m and 20m

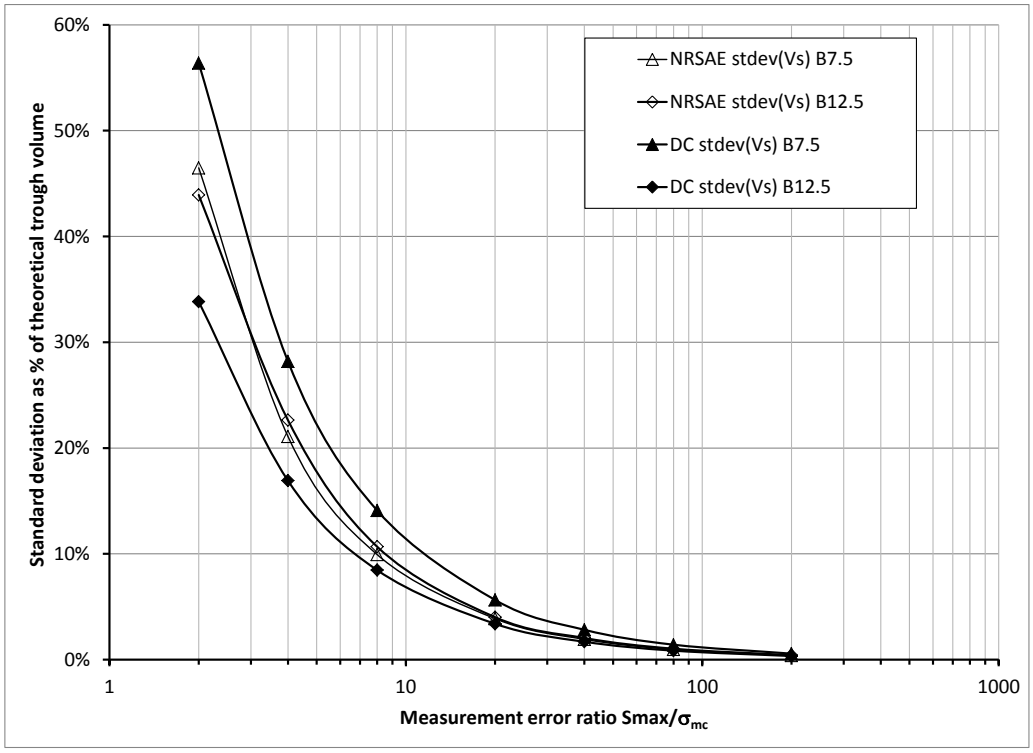

Figure 16: Monte Carlo standard deviation of trough volume as a percentage of theoretical trough volume for array type B, trough widths 7.5m and 12.5m

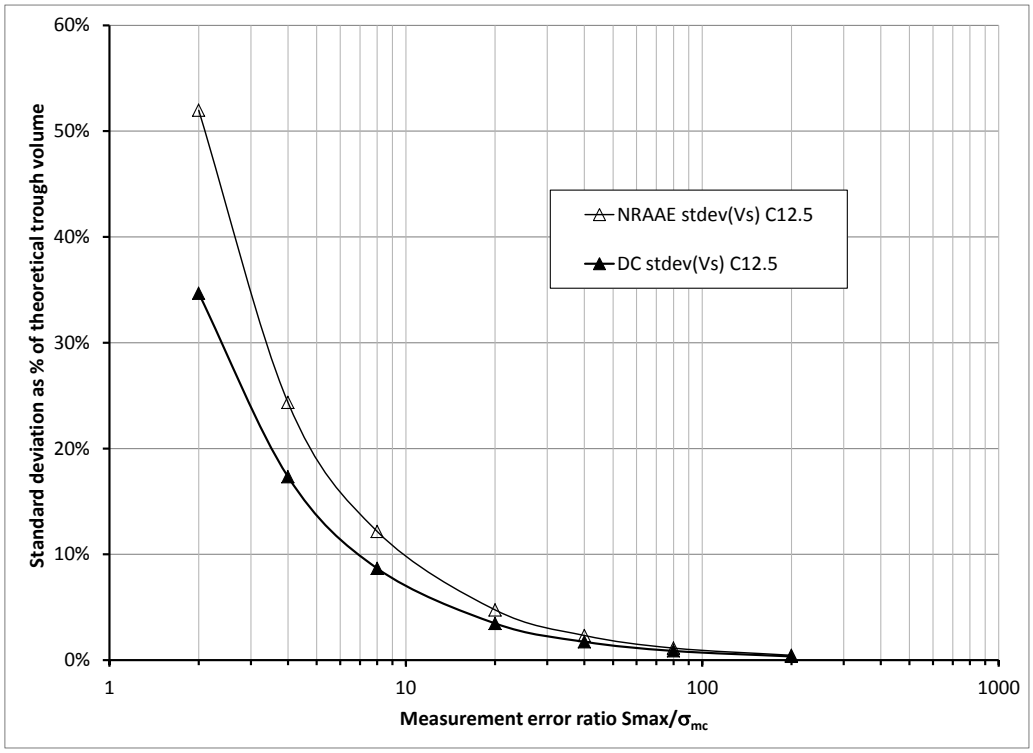

Figure 17: Monte Carlo standard deviation of trough volume as a percentage of theoretical trough volume for array type C, trough width 12.5m

2.5 Discussion of results of Monte Carlo analysis

Monte Carlo analysis is the only way in which the difference between various Gaussian curve-fitting methods could be compared in a rational, repeatable and quantifiable manner.

The results indicate that nonlinear regression is the best method to use for estimating trough width, with estimates of trough width following a lognormal distribution with a geometric mean close to the expected mean and a standard deviation lower than the other methods. On the other hand, direct calculation methods have computational advantages and do not require complex iterative calculations.

When using the nonlinear regression method on real data, the standard deviation of the trough width can be estimated based on Figures 5 to 10, and the standard deviation of trough volume can be estimated based on Figures 15 to 17.

For most practical purposes, the lowest error ratio to achieve acceptable estimates of Gaussian curve parameters is between 4 and 8. This corresponds to a maximum settlement of between 1 and 2 mm used with a monitoring method with a standard deviation of measurement error of 0.25 mm. This would roughly correspond to precise levelling with a repeatability of ± 0.5 mm with maximum settlements greater than 1 to 2 mm (depending on the configuration of the array and the trough width).

Accuracy may be improved by using arrays with more points. In particular, use of a settlement monitoring array with a configuration similar to array type A is not recommended, as multiple minima may occur in the nonlinear regression analysis, which makes convergence to a solution difficult.

3 CASE STUDY – HONOR OAK TO BRIXTON

The following chapter presents a detailed case study of surface settlements measured along the route of the Honor Oak to Brixton Thames Water Ring Main Extension tunnel. This tunnel was a 4.9 km long tunnel driven from Honor Oak in the London Borough of Southwark to Brixton in the London Borough of Lambeth. The 2.9 m I.D. tunnel was excavated by an Earth Pressure Balance (EPB) Tunnel Boring Machine (TBM) and surface settlements were measured for tunnel depths between 34.2 and 52.3 m. No surface settlements were recorded when the tunnel face was in the Chalk. Volume losses in other strata were between 0.16 and 1.13%.

3.1 Location, tunnelling method and geology

A location plan of the Honor Oak to Brixton Thames Water Ring Main Extension tunnel relative to the rest of the Thames Water Ring Main, and in particular the Stoke Newington to New River Head extension constructed at the same time, is shown in Figure 18.

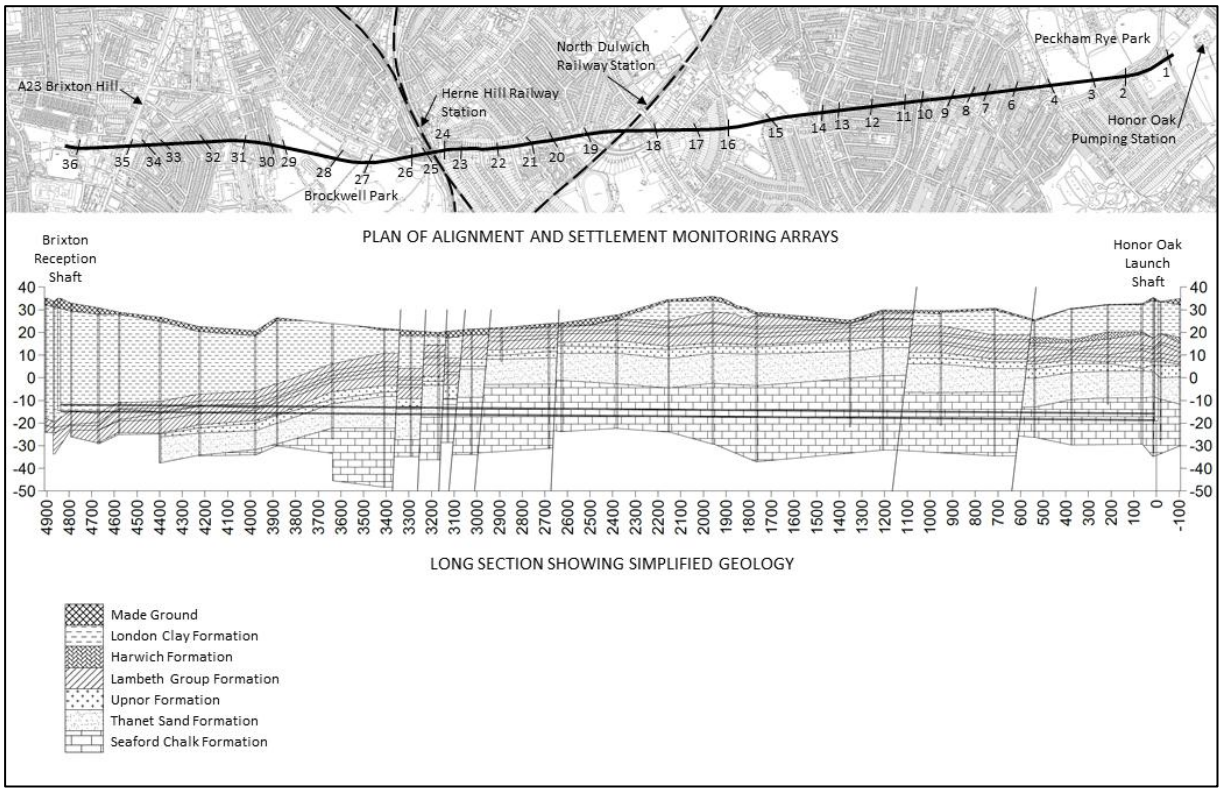

Figure 18: Plan and long section of Honor Oak to Brixton Thames Water Ring Main Extension tunnel

The 4.9 km long, 2.9 m I.D. tunnel was excavated by an Earth Pressure Balance (EPB) Tunnel Boring Machine (TBM) at depths between 34 and 52 m below the surface. The excavated diameter was 3.6 m. Within the tailskin, a 300 mm thick steel fibre reinforced precast concrete bolted segmental lining was erected and the annular gap was grouted using pressurised inert grout.

The tunnel was driven from a shaft near Honor Oak Reservoir, on the right hand side of Figure 18, just to the South of Peckham Rye Park, to a reception shaft near the Brixton pump out shaft of the Thames Water Ring Main, sandwiched between the A23 and Brixton Prison. Figure 18 shows the

tunnel to have been mainly driven through the Chalk, with approximately the final third of its length through the Thanet Sand, the Lambeth Group and then the London Clay.

3.2 Surface settlements

Surface settlements were monitored by precise levelling of fixed points arranged in transverse arrays. This gave feedback on the performance of the tunnelling process and mitigated risk to third parties. The following section describes the methods and procedures adopted for the precise levelling along the route, assesses the repeatability of the readings obtained and discusses the possible sources of the variability encountered. Then Gaussian settlement trough parameters *i* and V_s are calculated from the data.

3.2.1 Precise levelling procedure

A very similar precise levelling procedure was used for the Honor Oak to Brixton tunnel as for the Stoke Newington to New River Head tunnel (Jones, 2010). A Leica DNA03 level was used with a bar-coded Invar staff. Over the length of a levelling loop for a typical array this should result in a repeatability of less than ± 0.1 mm under controlled conditions according to the instrument manual (Leica Geosystems, 2009). However, a range of other factors such as ambient temperature, heavy traffic, sunlight heating the road or pavement surfacing and near-surface pore pressure changes due to rain or tree root suctions will result in a worse repeatability than this. These factors result in background movements, some of which will affect each monitoring point randomly and independently, and some of which will affect an array of monitoring points in a similar manner.

Road nails were installed in the road surface or pavement for use as monitoring points. Two benchmarks were used for each single point or array, one either side of the tunnel alignment, and at least 50 m from the tunnel centreline to ensure they were outside the zone of influence. Monitoring point levels were then baselined to both benchmarks using a weighted average depending on relative distance. This reduced systematic measurement errors and meant that if one benchmark was damaged, removed or parked over, levels could still be obtained.

There were 35 arrays (no.5 was removed before tunnelling began). The chainage was zero at the centre of Honor Oak shaft, increasing towards Brixton shaft. A list of settlement arrays is provided in Table 4.

Array	Depth to axis (m)	Face geology
1	51.7	Chalk
2	52.2	Chalk
3	50.2	Chalk
4	44.4	Chalk
6	48.6	Chalk
7	49.1	Chalk
8	49.2	Chalk
9	48.5	Chalk
10	47.3	Chalk
11	46.7	Chalk
12	45.2	Chalk
13	44.1	Chalk
14	43.1	Chalk
15	45.9	Chalk
16	52.0	Chalk
17	52.3	Chalk
18	44.6	Chalk
19	40.4	Chalk

Array	Depth to axis (m)	Face geology
20	38.2	Chalk
21	37.6	Chalk
22	36.6	Chalk
23	36.6	Chalk
24	34.9	TS
25	35.1	TS/UF
26	34.2	TS/UF
27	36.7	TS
28	39.4	TS
29	39.0	LMB
30	36.2	LMB/LSB
31	37.2	LMB/LSB
32	38.2	LMB/LSB/LTB
33	41.8	LMB/LTB
34	42.3	LTB/UMB/USB
35	41.8	LTB/UMB/USB
36	46.5	LCF

Key: TS = Thanet Sand, UF = Upnor Fm, LMB = Lower Mottled Beds, LSB = Lower Shelly Beds, LTB = Laminated Beds, UMB = Upper Mottled Beds, USB = Upper Shelly Beds, LCF = London Clay Fm.

Table 4: Locations of surface settlement arrays with recorded face geology.

3.2.2 Repeatability and variability in the field

Most of the monitoring points were levelled frequently well in advance of the TBM entering the zone of influence, and continued for a fairly long period after the TBM had passed the array. Therefore, a large number of readings were taken of each point. By examining the readings taken before the TBM was within 50m of each array, one can get an idea of the background movements. There were 1576 such readings taken, which represents a wealth of data to examine the stability of the points.

Assuming that the zone of influence was from 50 m before the array to 50 m past the array, then the 'baseline reading' has been taken as the last reading before the TBM was within 50 m of the array and the 'short term settlement' has been taken as the first reading after the TBM was more than 50 m past the array. 'Background readings' are all the readings taken before the TBM entered the zone of influence.

Stability of a monitoring point can be judged by visual inspection of the background readings. However, stability depends in part on how quickly the TBM will pass through the zone of influence. For instance, a point that is settling over several weeks at an average rate of 0.05 mm/day due to environmental effects can be assumed stable if the TBM passes through the zone of influence in 2-3 days, but cannot be assumed stable if the TBM passes through the zone of influence in 2 weeks. With the magnitudes of maximum settlement generally between 0 and 3 mm, a trend in the background readings that would result in an error of more than 0.5 mm between the time of the baseline reading and the short term settlement was defined as significant and the data treated with caution. If the trend would result in an error of more than 1.0 mm the point was ignored in the interpretation. Similarly, monitoring points that did not show a definite trend during the baseline readings, but exhibited large fluctuations in the readings of more than +/- 0.5 mm, were treated with caution.

The background readings for all the monitoring points are shown in Figure 19 as traces. There were 174 monitoring points in total, of which 169 are shown because Array 1 couldn't be considered to have background readings, being so close to the launch shaft, which was being constructed at the time they were installed. Most of the readings were within +/- 1 mm, even for over 100 days, showing that even seasonal environmental effects on the scale of weeks or months were not causing them to move significantly. However, there were a few that were clearly very unstable with one settling 24mm over about 100 days.

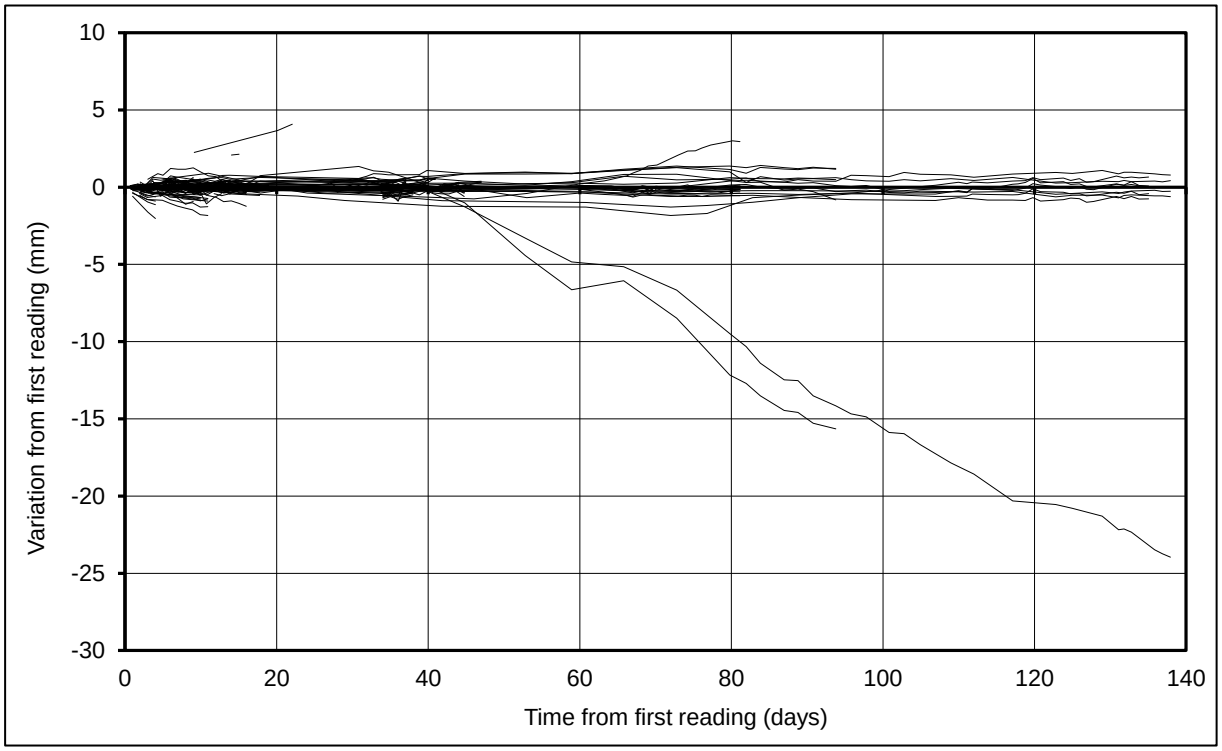

Figure 19: Background readings for all Honor Oak to Brixton surface settlement monitoring points

3.2.3 Calculation of surface settlement trough parameters

Gaussian curves have been fit to the data using a nonlinear regression method (NRSAE). Volume loss and trough width were both varied until the minimum sum of the absolute errors was found, as described in Section 2.2.3.

3.2.4 Surface settlements when tunneling through the Chalk

The calculated surface settlement trough parameters for the arrays where the tunnel face was in the Chalk are listed in Table 5.

Array no. (chainage)	Volume loss V_s	Trough width parameter K	Maximum settlement S_{max}	Depth to tunnel axis
Array 1 (32)	0.0 %	Not measurable	0.0 mm	51.7 m
Array 2 (236)	0.0 %	Not measurable	0.0 mm	52.2 m
Array 3 (373)	0.0 %	Not measurable	0.0 mm	50.3 m
Array 4 (552)	0.0 %	Not measurable	0.0 mm	44.4 m
Array 6 (711)	0.0 %	Not measurable	0.0 mm	48.6 m
Array 7 (822)	0.0 %	Not measurable	0.0 mm	49.1 m
Array 8 (904)	0.0 %	Not measurable	0.0 mm	49.2 m
Array 9 (989)	0.0 %	Not measurable	0.0 mm	48.5 m
Array 10 (1116)	0.0 %	Not measurable	0.0 mm	47.3 m
Array 11 (1195)	0.0 %	Not measurable	0.0 mm	46.7 m
Array 12 (1335)	0.0 %	Not measurable	0.0 mm	45.2 m
Array 13 (1472)	0.0 %	Not measurable	0.0 mm	44.1 m
Array 14 (1563)	0.0 %	Not measurable	0.0 mm	43.1 m
Array 15 (1805)	0.0 %	Not measurable	0.0 mm	45.9 m
Array 16 (1970)	0.0 %	Not measurable	0.0 mm	52.0 m
Array 17 (2091)	0.0 %	Not measurable	0.0 mm	52.3 m
Array 18 (2266)	0.0 %	Not measurable	0.0 mm	44.6 m
Array 19 (2563)	0.0 %	Not measurable	0.0 mm	40.4 m
Array 20 (2667)	0.0 %	Not measurable	0.0 mm	38.2 m
Array 21 (2818)	0.0 %	Not measurable	0.0 mm	37.6 m
Array 22 (2965)	0.0 %	Not measurable	0.0 mm	36.6 m

Table 5: Surface settlement trough parameters – tunnel face in the Chalk

Table 5 shows clearly that there were no discernible surface settlements when the tunnel face was in the Chalk. This is an important result for the feasibility of future tunnelling projects in the Chalk.

3.2.5 Surface settlements when tunnelling through strata above the Chalk

The settlement monitoring data and fitted surface settlement trough curves for tunnelling through strata above the Chalk are shown in Figures 20 to 33, and the settlement trough parameters are summarised in Table 6.

Array no. (chainage)	Volume loss V_s	Trough width i	Trough width parameter K	Maximum settlement S_{max}	Average absolute error	Depth to tunnel axis
Array 23 (3113)	0.44 %	17.7 m	0.484	1.0 mm	0.045 mm	36.6 m
Array 24 (3200)	0.16 %	9.0 m	0.258	0.7 mm	0.074 mm	34.9 m
Array 25 (3275)	0.85 %	22.1 m	0.630	1.5 mm	0.105 mm	35.1 m
Array 26 (3334)	0.54 %	22.4 m	0.655	1.0 mm	0.124 mm	34.2 m
Array 27 (3525)	0.22 %	27.6 m	0.752	0.3 mm	0.087 mm	36.7 m
Array 28 (3663)	0.28 %	14.3 m	0.363	0.8 mm	0.080 mm	39.4 m
Array 29 (3898)	Unstable benchmark when TBM passing					39.0 m
Array 30 (3955)	1.13 %	15.2 m	0.420	3.0 mm	0.126 mm	36.2 m
Array 31 (4071)	2 unstable points when TBM passing					37.2 m
Array 32 (4251)	0.90 %	22.3 m	0.584	1.6 mm	0.099 mm	38.2 m
Array 33 (4413)	0.29 %	13.3 m	0.318	0.9 mm	0.053 mm	41.8 m
Array 34 (4494)	0.62 %	16.8 m	0.397	1.5 mm	0.131 mm	42.3 m
Array 35 (4585)	2 unstable points when TBM passing					41.8 m
Array 36 (4783)	2 unstable points when TBM passing					46.5 m

Notes: Array 34 – point E at +25m offset was unstable, so this point was ignored.

Table 6: Surface settlement trough parameters – tunnel face in strata above the Chalk

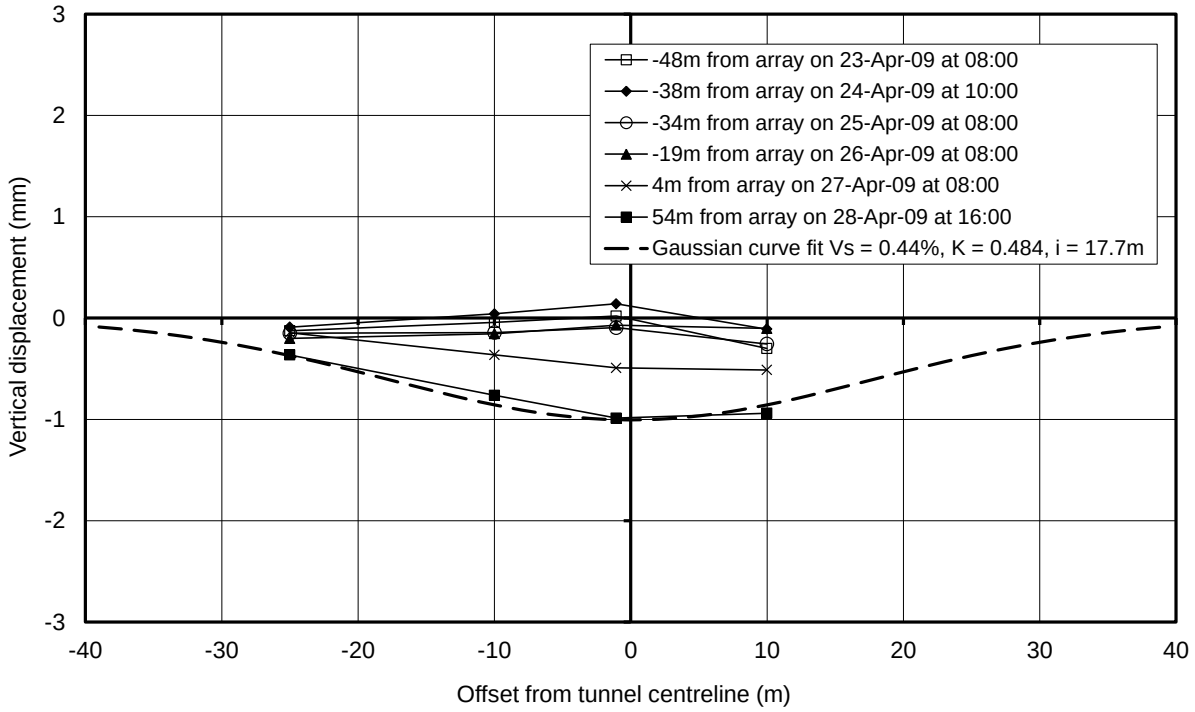

Figure 20: Honor Oak to Brixton Array 23 surface settlements

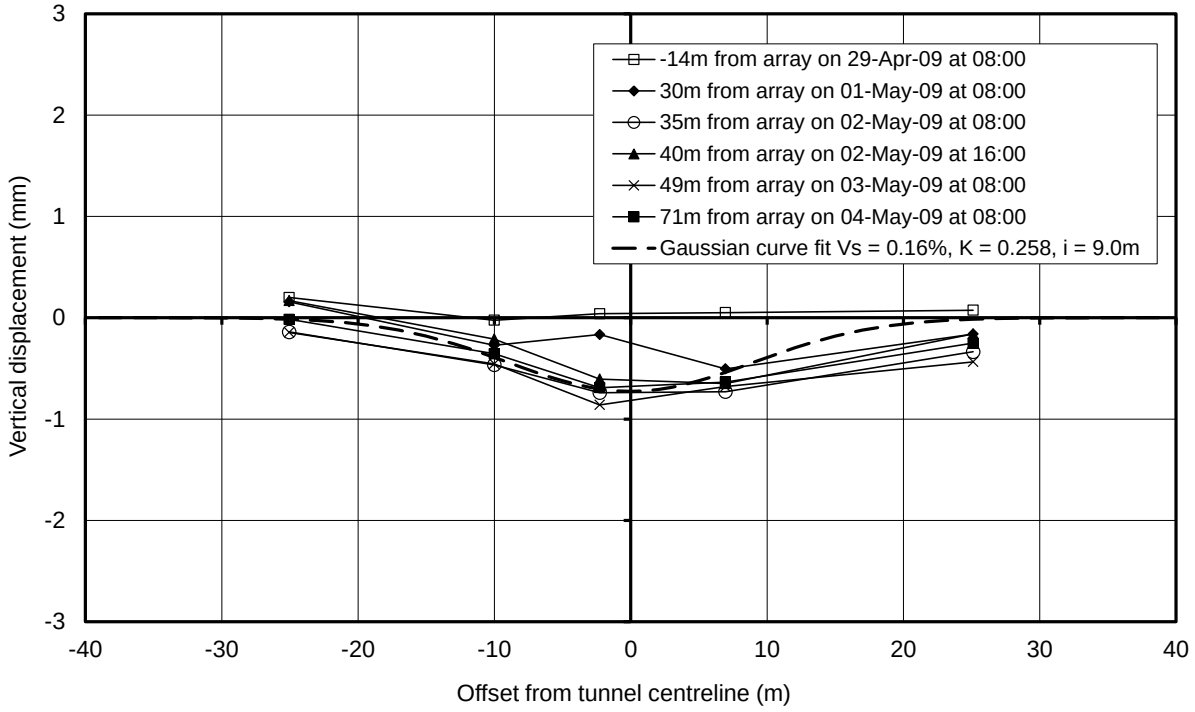

Figure 21: Honor Oak to Brixton Array 24 surface settlements

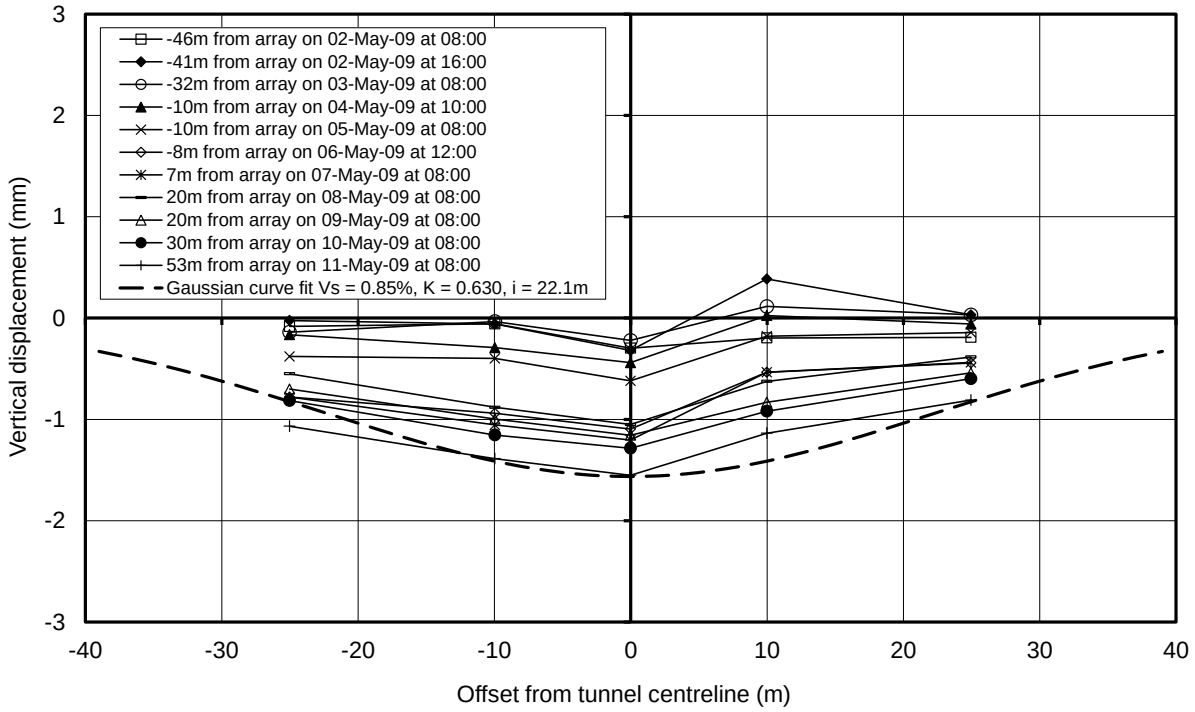

Figure 22: Honor Oak to Brixton Array 25 surface settlements

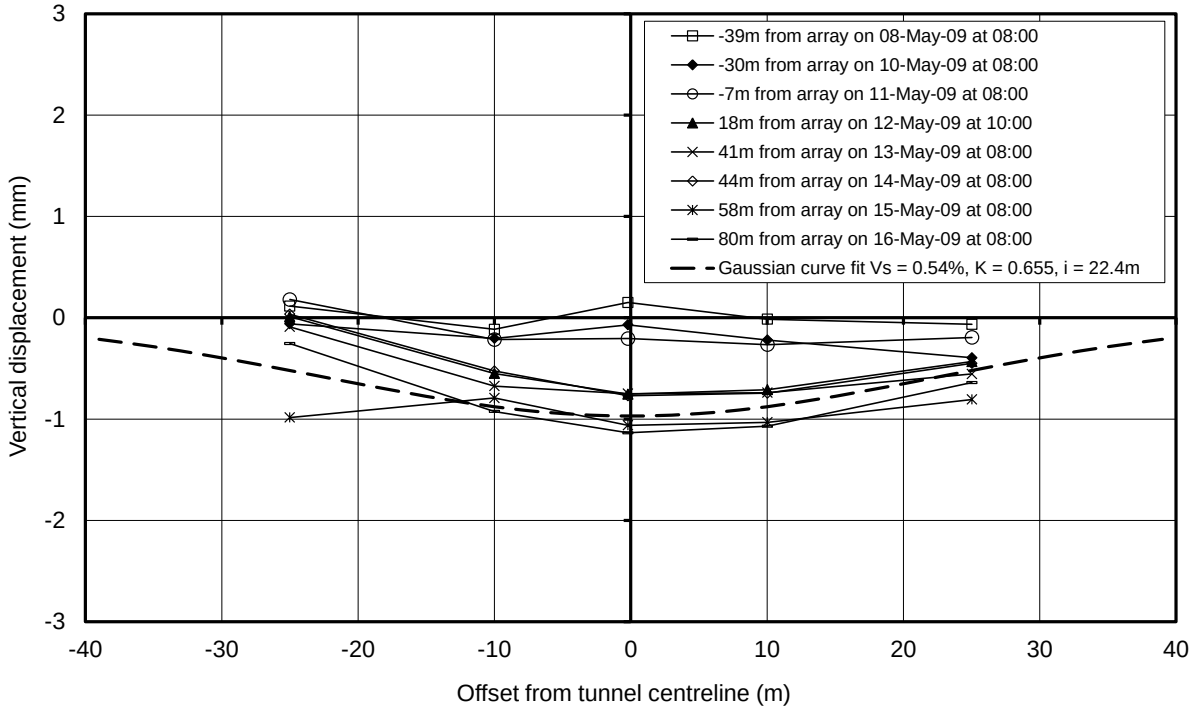

Figure 23: Honor Oak to Brixton Array 26 surface settlements

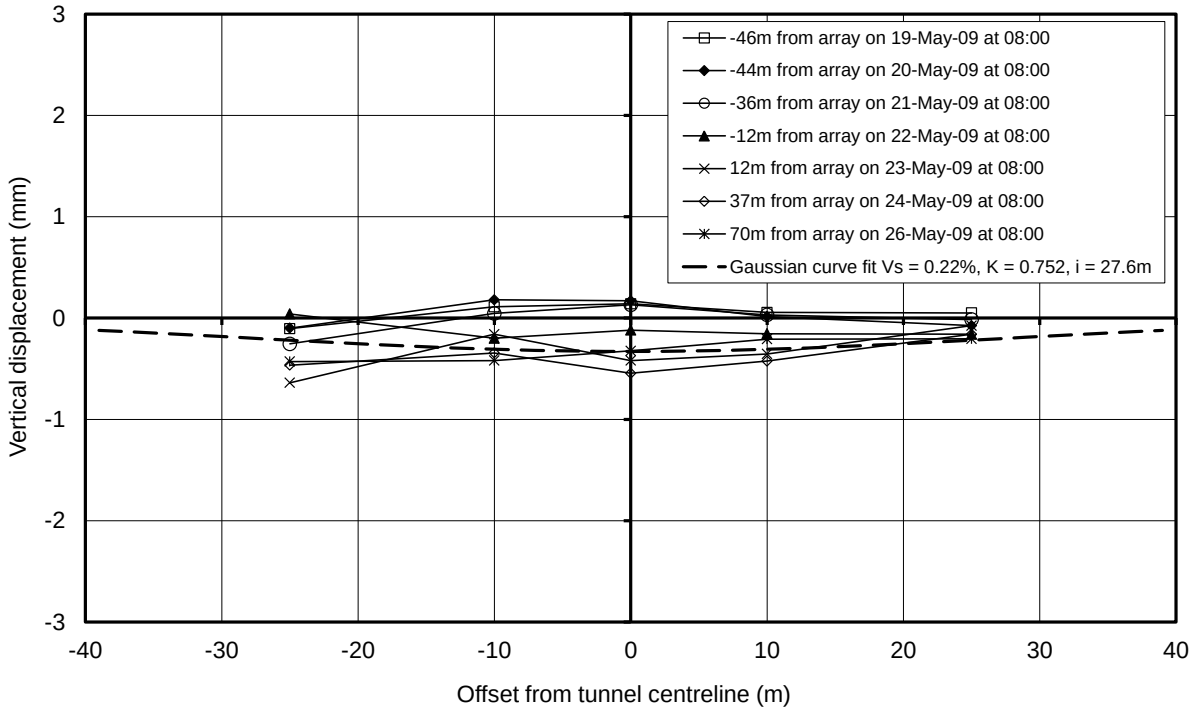

Figure 24: Honor Oak to Brixton Array 27 surface settlements

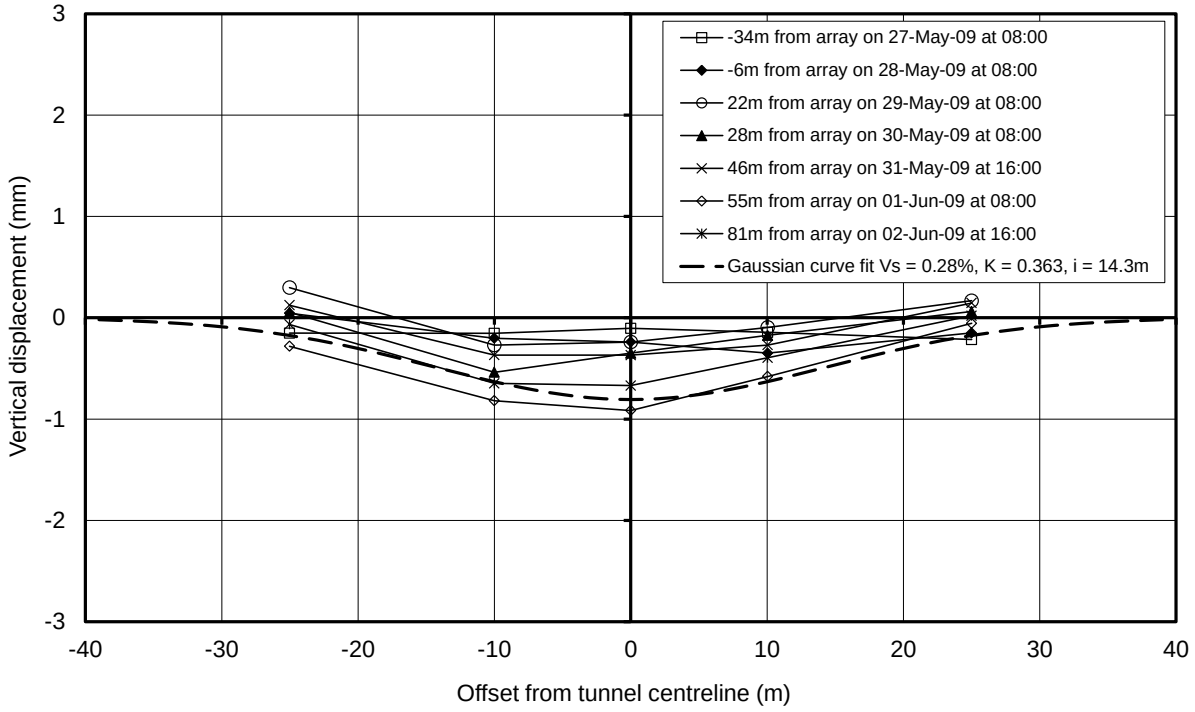

Figure 25: Honor Oak to Brixton Array 28 surface settlements

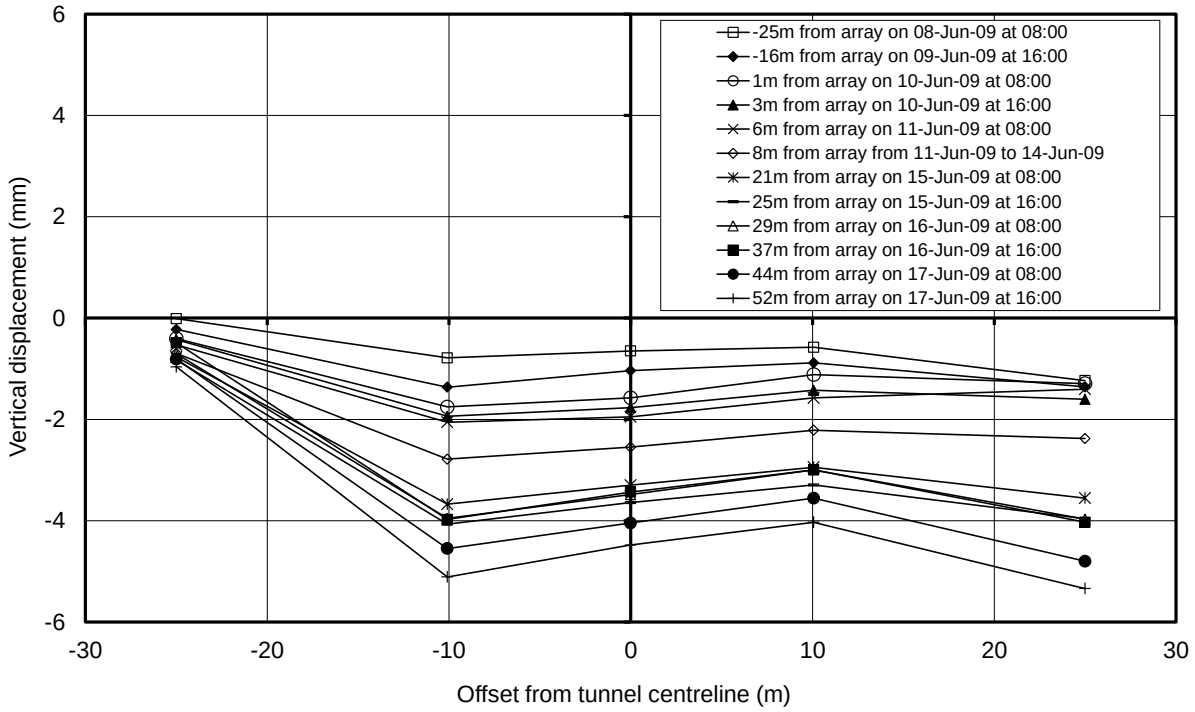

Figure 26: Honor Oak to Brixton Array 29 surface settlements

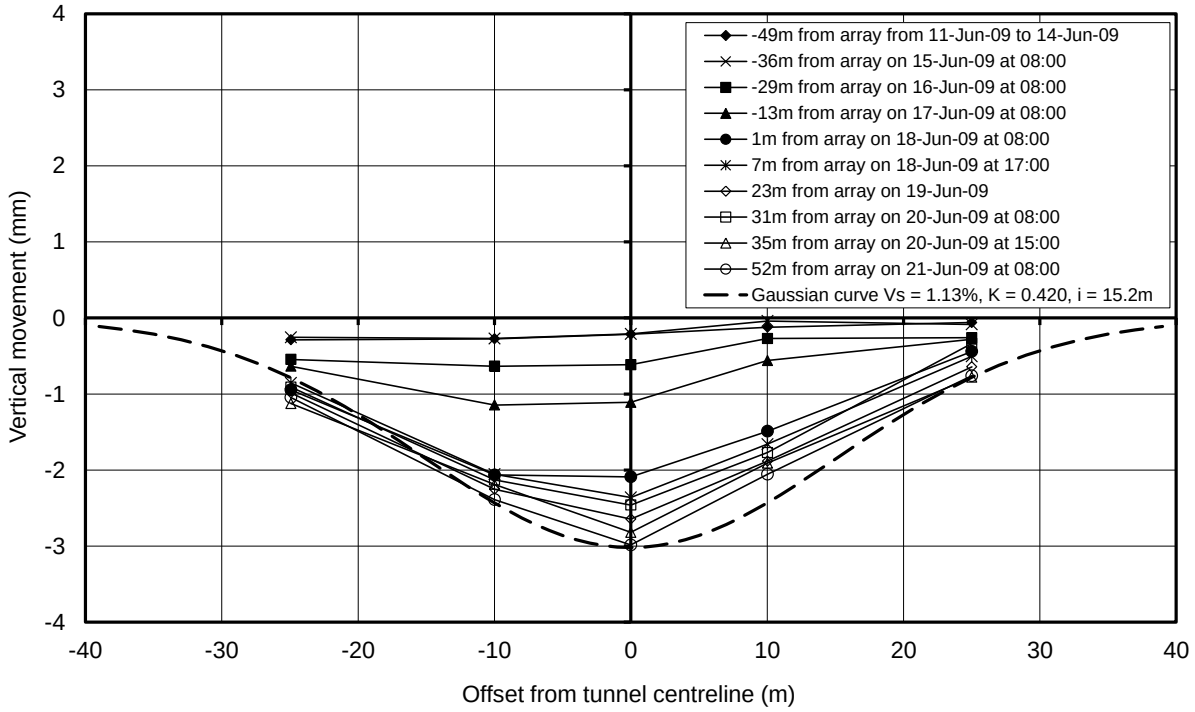

Figure 27: Honor Oak to Brixton Array 30 surface settlements

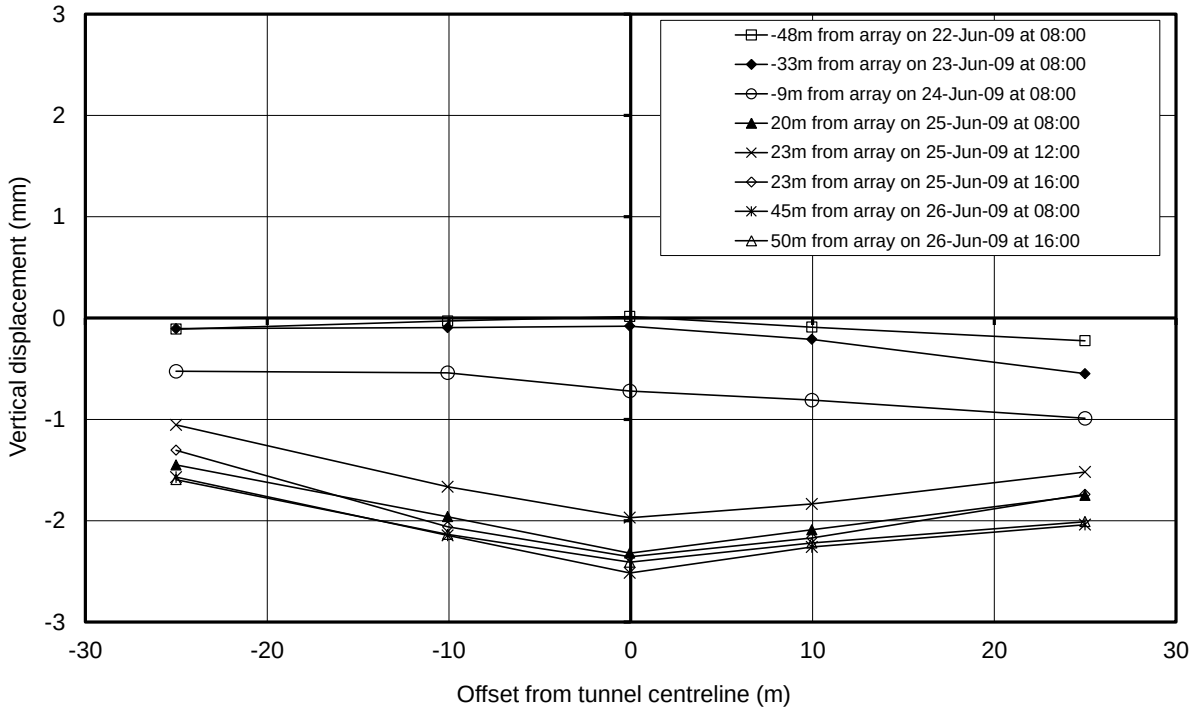

Figure 28: Honor Oak to Brixton Array 31 surface settlements

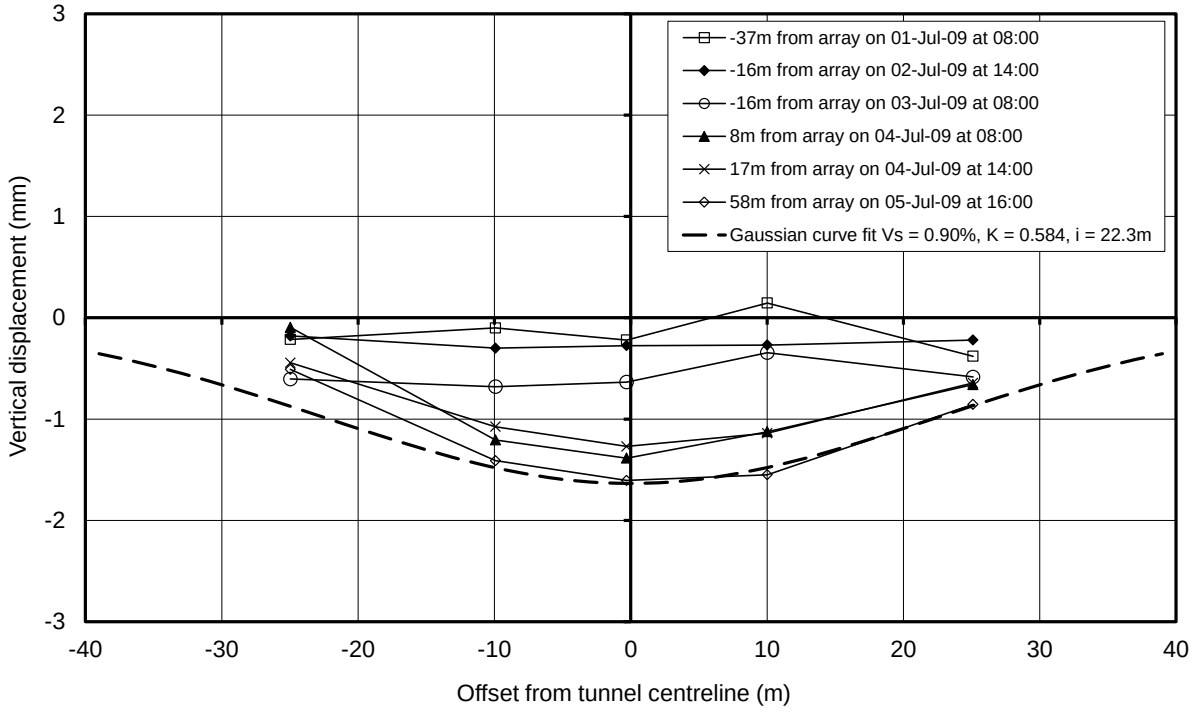

Figure 29: Honor Oak to Brixton Array 32 surface settlements

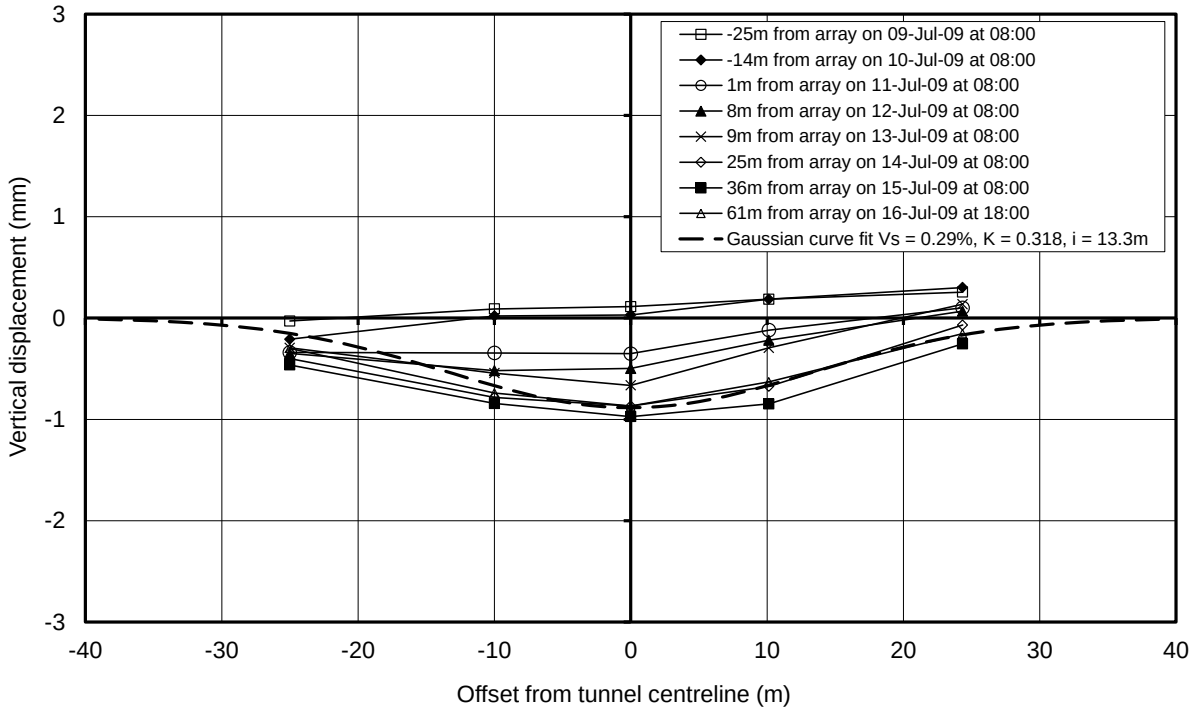

Figure 30: Honor Oak to Brixton Array 33 surface settlements

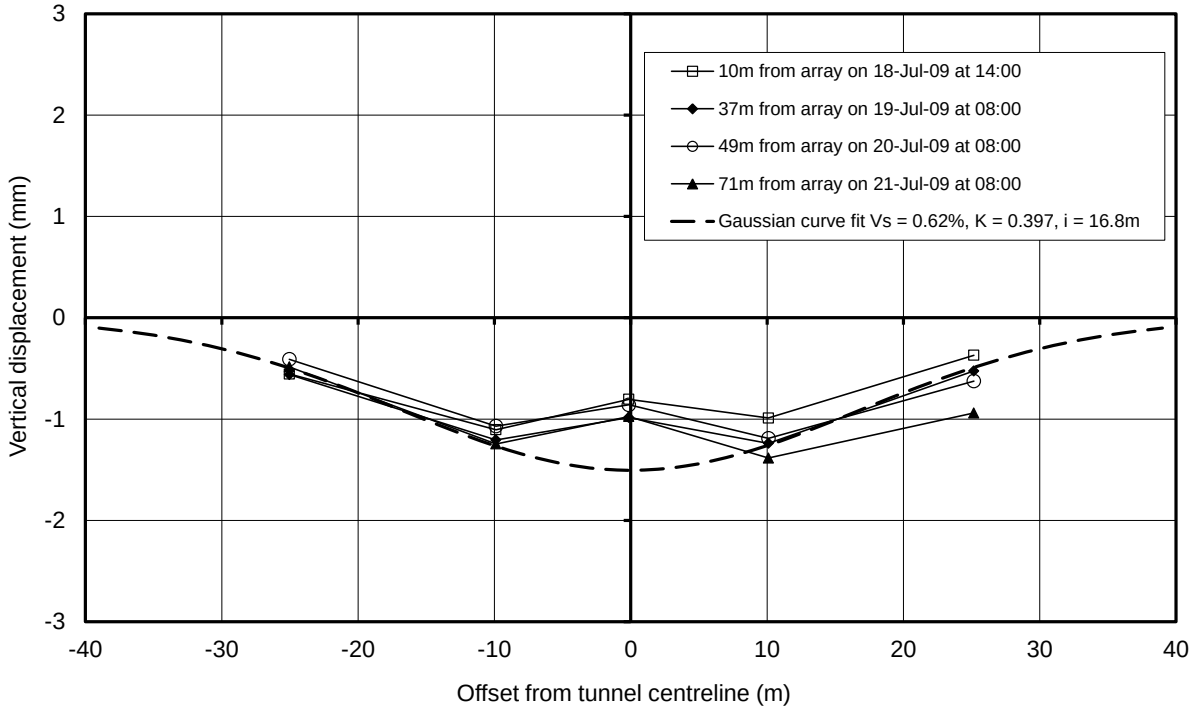

Figure 31: Honor Oak to Brixton Array 34 surface settlements

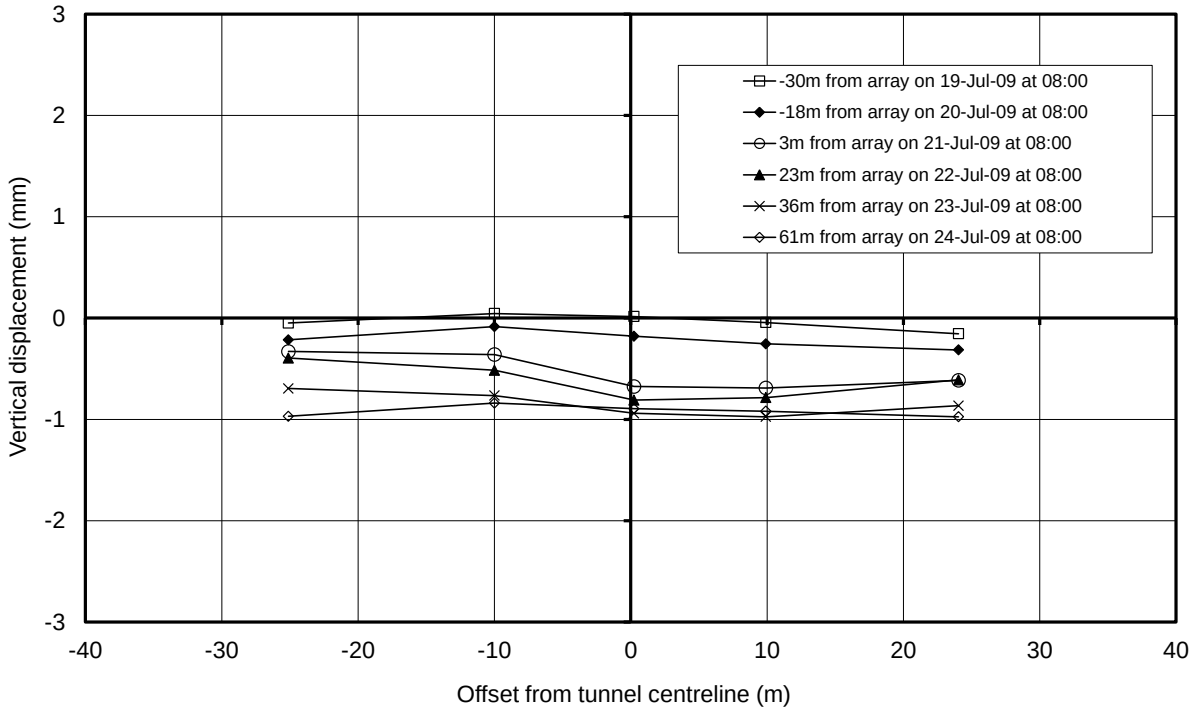

Figure 32: Honor Oak to Brixton Array 35 surface settlements

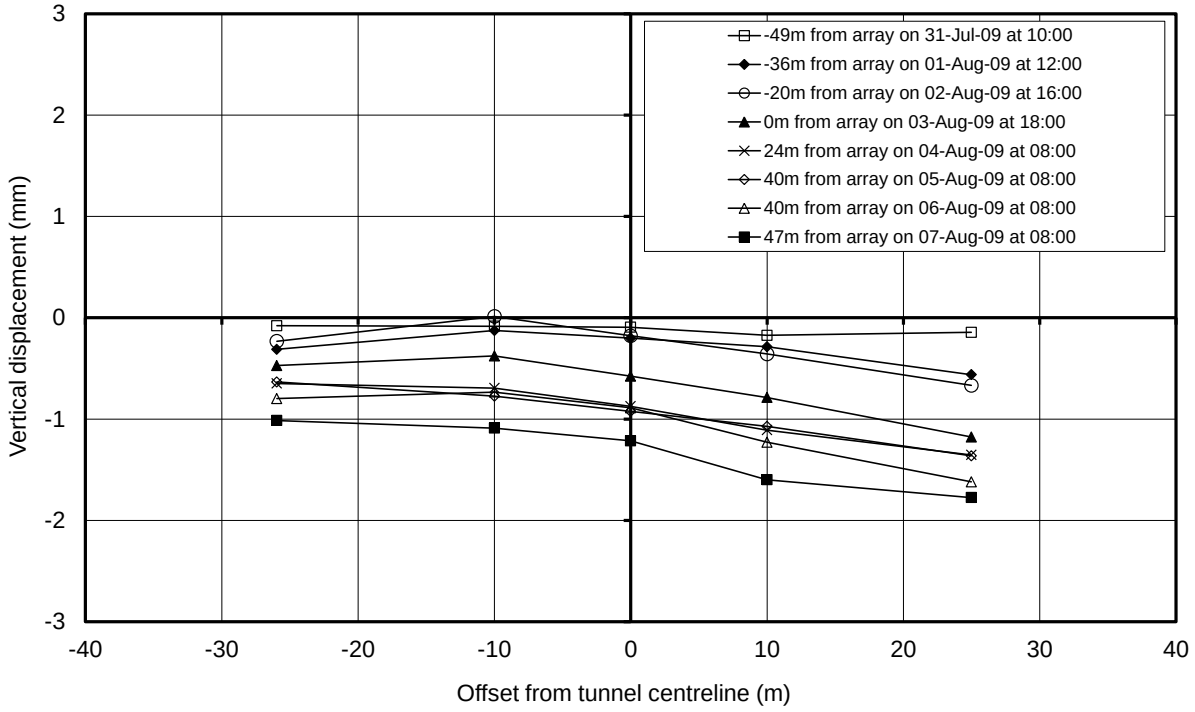

Figure 33: Honor Oak to Brixton Array 36 surface settlements

Table 5 shows clearly that the Chalk was stiff enough and strong enough that tunnelling through it did not induce any ground movements large enough that they could be measured at the surface. As soon as the TBM came out of the chalk and entered the relatively softer deposits in the strata above, ground movements could be measured at the surface. In terms of the Load Factor, defined by Mair et al. (1981) as the ratio of stability ratio to critical stability ratio, tunnelling in the Chalk may have a Load Factor between 0.01 and 0.1, compared to a Load Factor of around 0.2 for EPB tunnelling in the non-chalk deposits.

Table 6 shows quite a large variation in volume loss and trough width values in the strata above the Chalk. There was no correlation between volume loss or trough width and the depth of the tunnel, and no correlation with any known feature of geology either in the face or above the tunnel. The higher volume losses did not correspond with fault zones, water pressures or any particular stratum. Unfortunately records of the face pressures applied during construction were not available; this may have been an important factor.

3.3 Summary

This chapter has shown that EPB tunnelling in the Chalk at depths to axis of between 36.6 and 52.3 m below ground level did not cause any discernible surface settlement, therefore volume losses were effectively 0.0 %.

Tunnelling through the relatively softer deposits of the Thanet Sand, Upnor, Lambeth Group and London Clay Formations at depths to axis of between 34.2 and 42.3 m did cause tunnelling-induced surface settlements. Volume losses were calculated at between 0.16 and 1.13 %. The range of depths was not very large, and no correlation was observed between trough width parameter *K* and depth on this project. The mean value of *K* was 0.486 and the standard deviation was 0.162.

The monitoring systems employed on the Thames Water Ring Main Extension Honor Oak to Brixton project were adequate mitigation for the risks. This case study is a valuable addition to the available literature on surface settlements in the Chalk, particularly since there are so few case histories available and predictions of volume loss are often conservative as a result. The section of tunnel that passed through the Thanet Sand, Upnor, Lambeth Group and London Clay Formations was deeper than nearly all published case histories in these strata, and therefore is of value in augmenting the otherwise rich database.

The variability of *K* measured in the field over a large number of projects appears to be fairly high, and sensitivity analyses should always be performed where *K* is a critical parameter.

4 REINTERPRETATION OF STOKE NEWINGTON TO NEW RIVER HEAD DATA

The settlement data from the Stoke Newington to New River Head Thames Water Ring Main Extension project, formerly published in Jones (2010), is reinterpreted in this chapter. At the time, due to a visually poor fit to the data from a trial with a nonlinear regression least squares (NRLS) analysis on one array, a direct calculation method (DCJ) was developed and used instead. Since then, Monte Carlo analyses (presented in Chapter 2) have shown that the nonlinear regression sum of absolute errors (NRSAE) method should be a more reliable method of curve-fitting than DCJ.

4.1 Comments on the reliability of Gaussian curve parameters obtained by curve-fitting for the Stoke Newington to New River Head tunnel

The repeatability of the precise levelling on the Stoke Newington to New River Head project was better than ± 0.5 mm, therefore a standard deviation of approximately 0.25 mm could be inferred as a worst case. The maximum settlements were between 0.4 and 1.9 mm, the trough widths were approximately in the range 7.5 m to 12.5 m, and most monitoring arrays were similar to array type B.

Therefore, looking up the DCJ values in Figure 8 and Figure 9 predicts a standard deviation of around 2.5 m for trough width. For an average trough width of 10m and at a tunnel depth of 50m, this would correspond to a standard deviation on trough width parameter of 0.05. It is highly unlikely that this error could explain the large disparity between the Stoke Newington to New River Head data and established empirical methods of predicting trough width such as those published by O'Reilly & New (1982) and Mair et al. (1993). The subsurface data presented in Jones (2010) provides further evidence in support of the hypothesis that trough width parameter is significantly overpredicted using established methods at depths greater than 35m.

Figure 8 and Figure 9 also showed that the DCJ method may systematically underpredict trough width, particularly as the trough gets wider, for some configurations of monitoring arrays.

Figure 16 indicates that the standard deviation of the volume loss estimates should have been 10 to 20 %. However, the accuracy of the direct calculation method used for the Stoke Newington to New River Head data should have been better than that used in the Monte Carlo analysis in Chapter 2, because considerable care was taken to ignore errors at large offsets.

4.2 Reinterpretation of surface settlement data

A reinterpretation of arrays where Gaussian curve parameters were measured is presented in Figure 34, Figure 35, Figure 36, Figure 37, Figure 38, Figure 39 and Figure 40.

In most cases the curves fit in a similar way. One exception is Figure 34 (Array 4300) and this illustrates the difference between how the curve-fitting methods work. The nonlinear regression method (NRSAE) has opted to fit the curve as close as possible to all the points except the centreline settlement point. This is because the sum of absolute errors is minimised in this state. The direct calculation method (DCJ) depends on trapezoidal integration to find the volume loss, which is then fixed, and then the trough width is calculated from the data. Therefore the volume loss and trough width calculations are uncoupled in the DCJ method, whereas in the NRSAE method they are coupled together as both are varied to find the best fit.

Figure 40 shows a rare case where the NRSAE method has failed to converge on a solution. Effectively the trough width and trough volume approached infinity due to the very flat shape of the settlement trough measured. It is probably not sensible to attempt to determine Gaussian curve parameters from data exhibiting this kind of pattern.

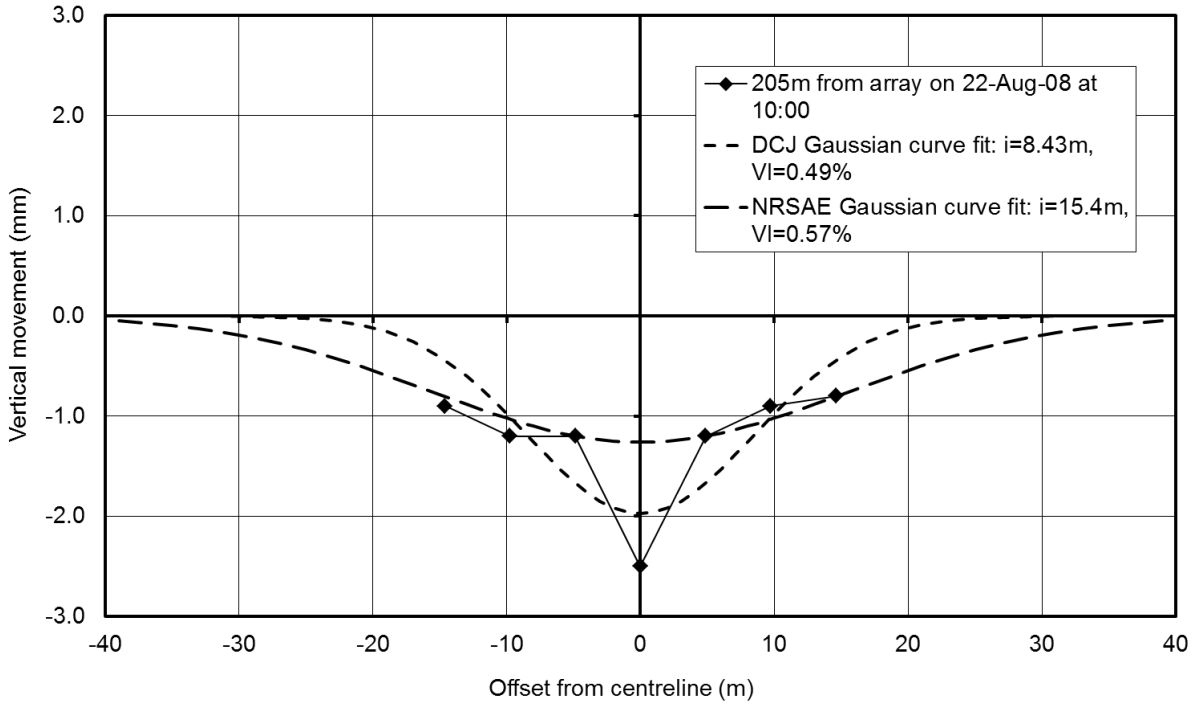

Figure 34: Stoke Newington to New River Head Array 4300 surface settlements

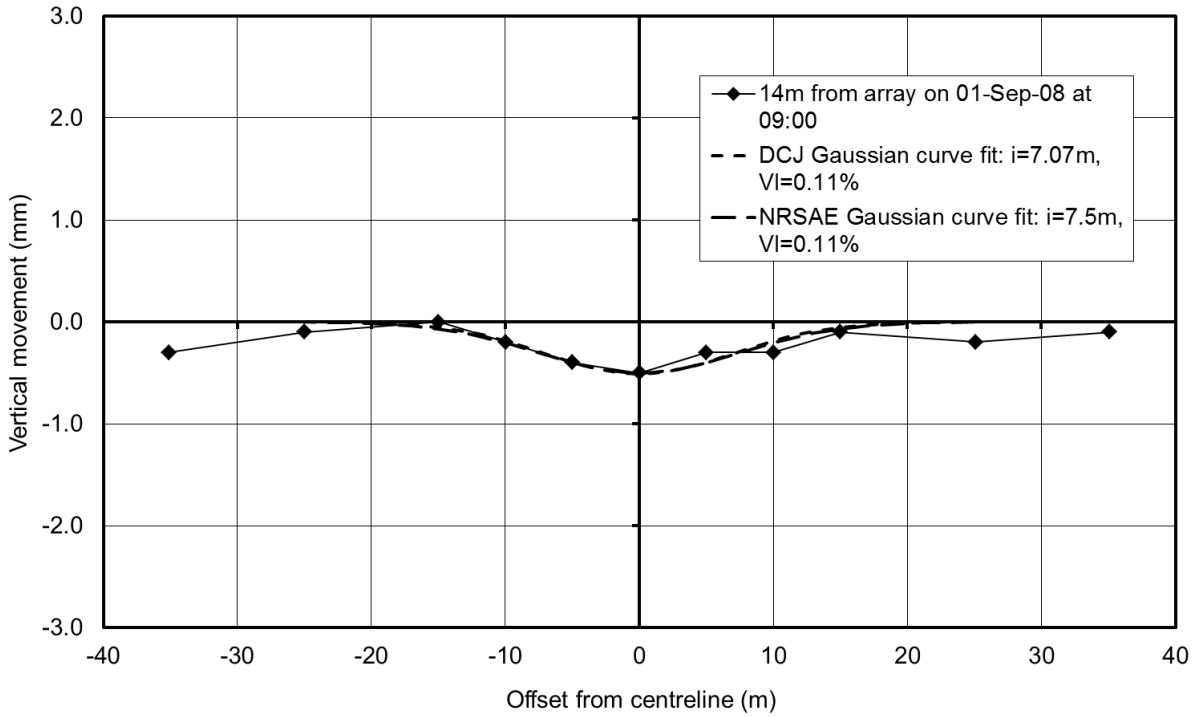

Figure 35: Stoke Newington to New River Head Array 3975 surface settlements

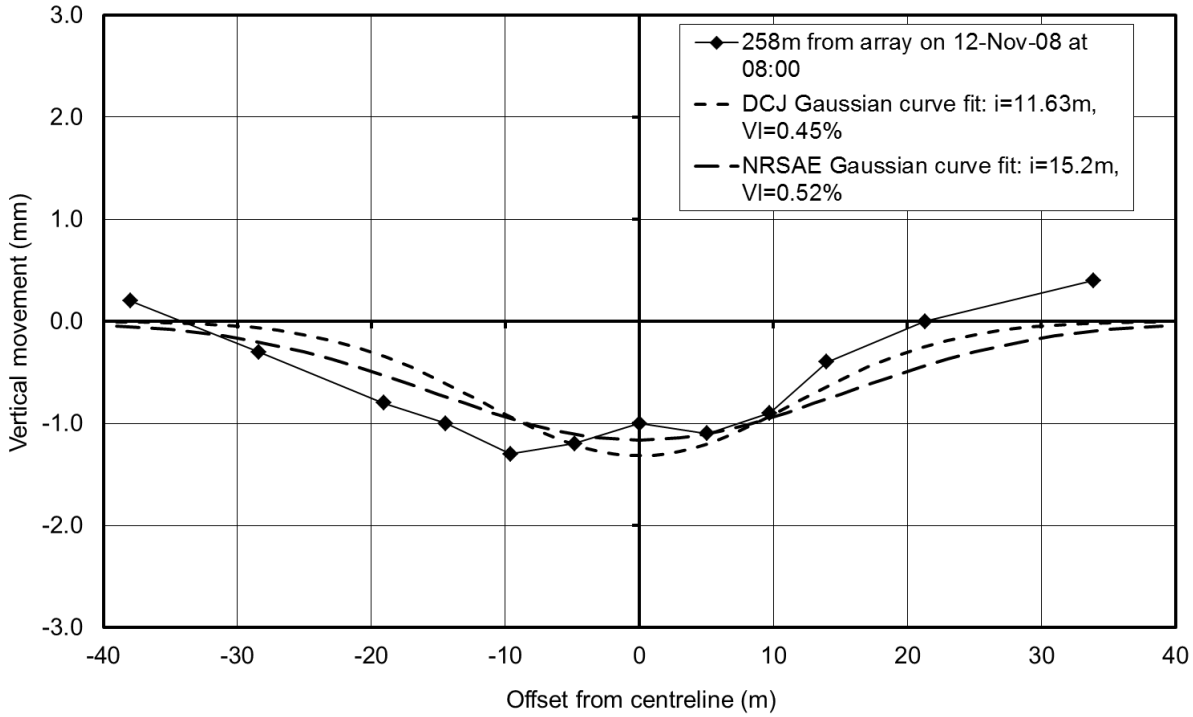

Figure 36: Stoke Newington to New River Head Array 3060 surface settlements

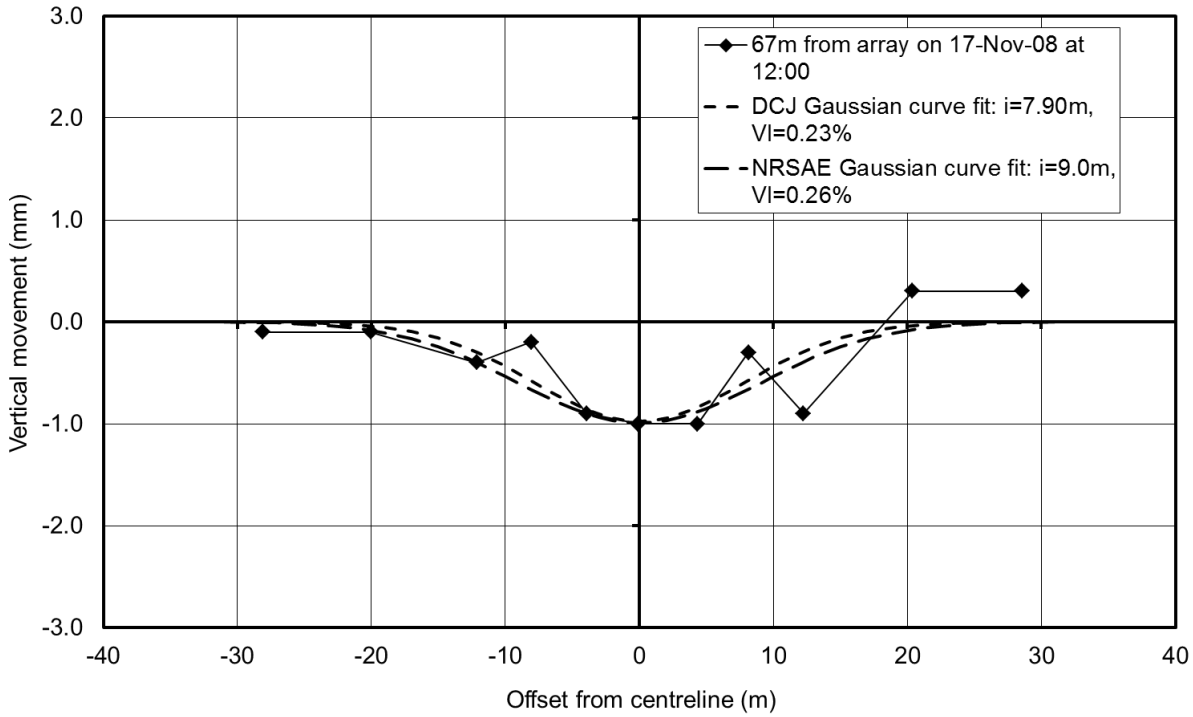

Figure 37: Stoke Newington to New River Head Array 2800 surface settlements

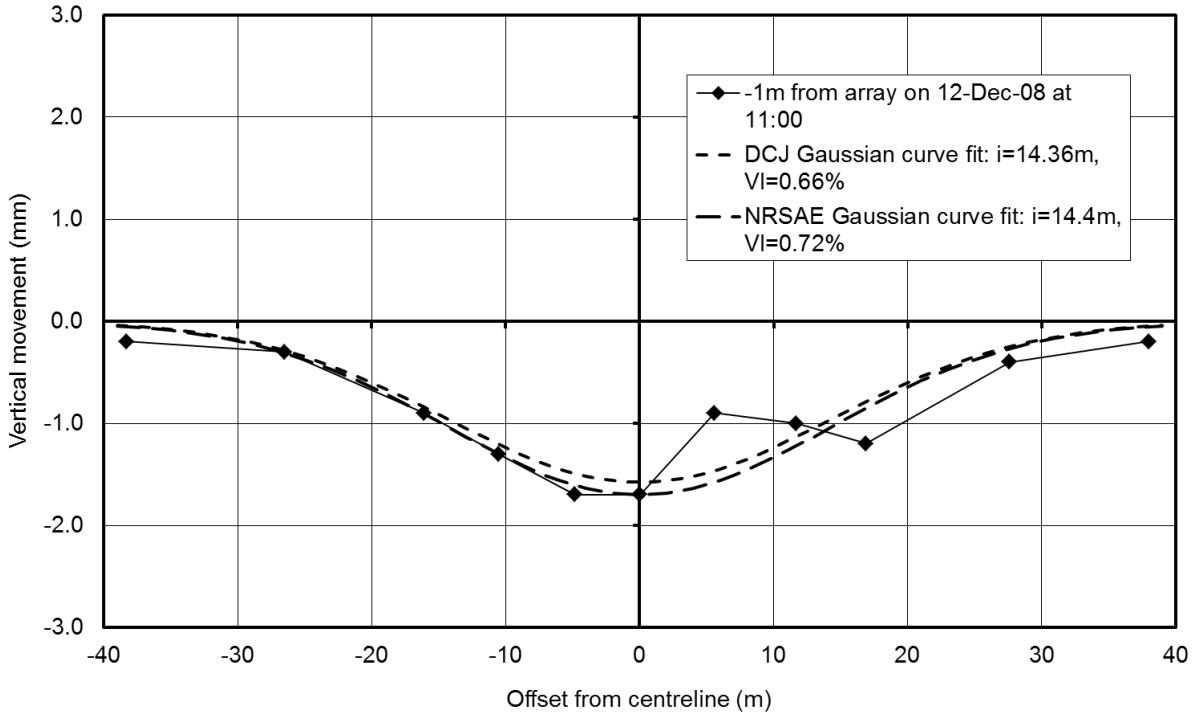

Figure 38: Stoke Newington to New River Head Array 2470 surface settlements

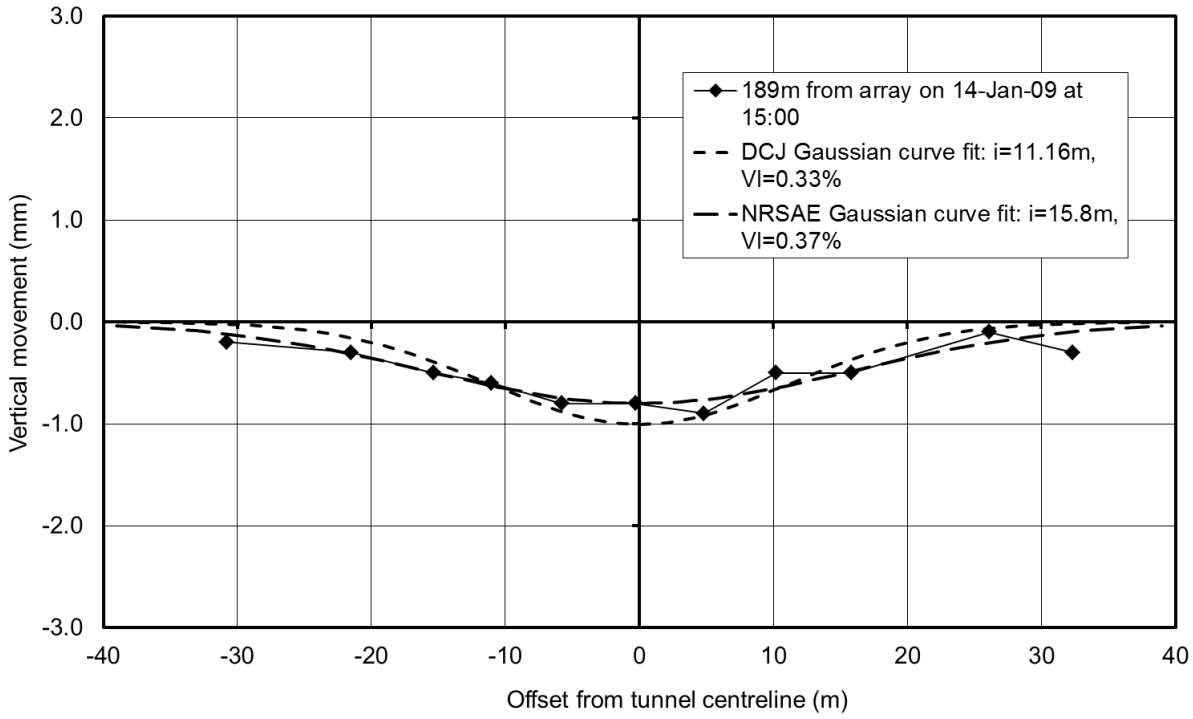

Figure 39: Stoke Newington to New River Head Array 2150 surface settlements

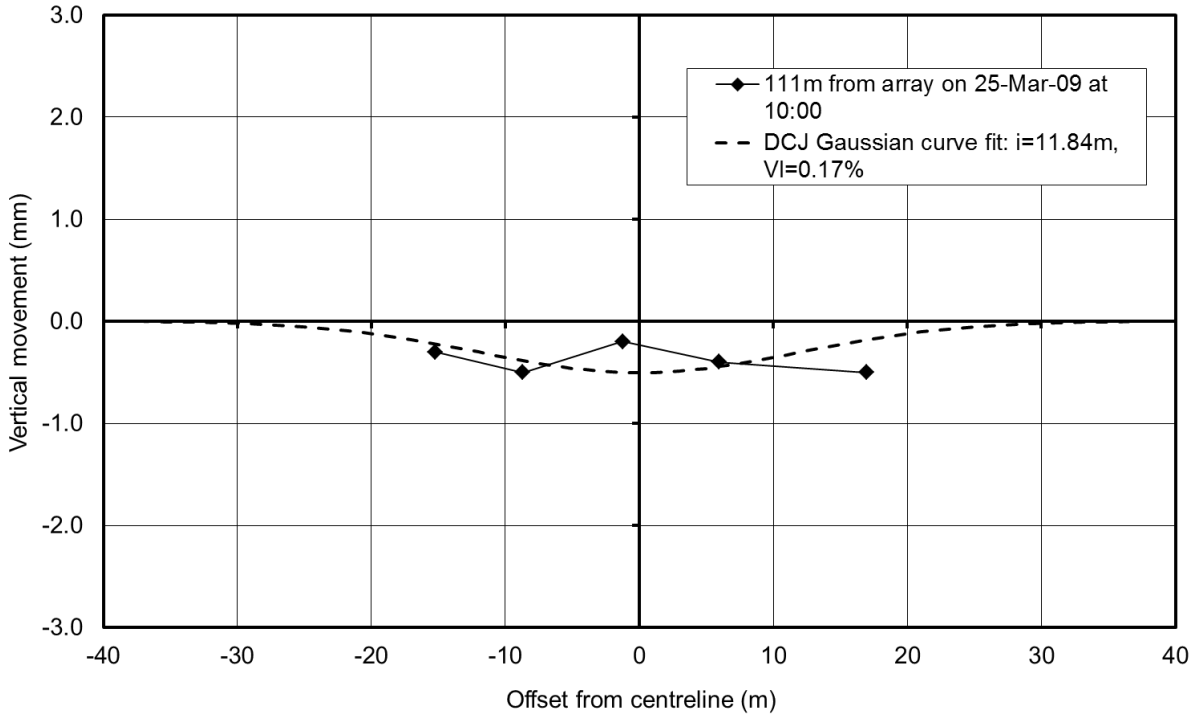

Figure 40: Stoke Newington to New River Head Array 730 surface settlements

4.3 Summary

A summary of the reinterpreted Gaussian curve parameters is shown in Table 7. As mentioned previously the curve-fitting methods got very different results for Array 4300. In addition, Table 7 shows that the NRSAE method found significantly wider troughs for Arrays 3060 and 2150. This appears to have been mainly due to the uncoupling of the trough volume and trough width calculations in the DCJ method. It is difficult, therefore, to know which values are 'better', since the Monte Carlo analysis showed that a direct trapezoidal integration was the most reliable method of calculating trough volume. However, it could also be argued that if 'best fit' is defined as the minimum sum of residuals, then by definition best fit is obtained by nonlinear regression.

The increase in trough width obtained through the use of the NRSAE method only slightly diminishes the large disparity between the Stoke Newington to New River Head data and established empirical methods of predicting trough width such as those published by O'Reilly & New (1982) and Mair et al. (1993). Therefore, the conclusion that these established methods underpredict trough width at depths greater than 35m is still valid.

Array	Depth to axis (m)	DC volume loss V_l (%)	DCJ trough width i (m)	DCJ trough width parameter K	NRSAE volume loss V_l (%)	NRSAE trough width i (m)	NRSAE trough width parameter K
4300	38.5	0.49	8.4	0.219	0.57	15.4	0.400
3975	38.2	0.11	7.1	0.185	0.11	7.5	0.196
3060	58.5	0.45	11.6	0.199	0.52	15.2	0.260
2800	58.8	0.23	7.9	0.134	0.26	9.0	0.153
2470	54.1	0.66	14.4	0.265	0.72	14.4	0.266
2150	50.9	0.33	11.2	0.219	0.37	15.8	0.310

Table 7: Gaussian curve parameters for Stoke Newington to New River Head surface settlement data: comparison of DCJ and NRSAE curve-fitting methods

5 DISCUSSION

To put the Honor Oak to Brixton data into context, the surface settlements have been plotted against height above the tunnel in Figure 41, along with other published case studies of tunnels in clays, and the logarithmic relationship proposed in Jones (2010).

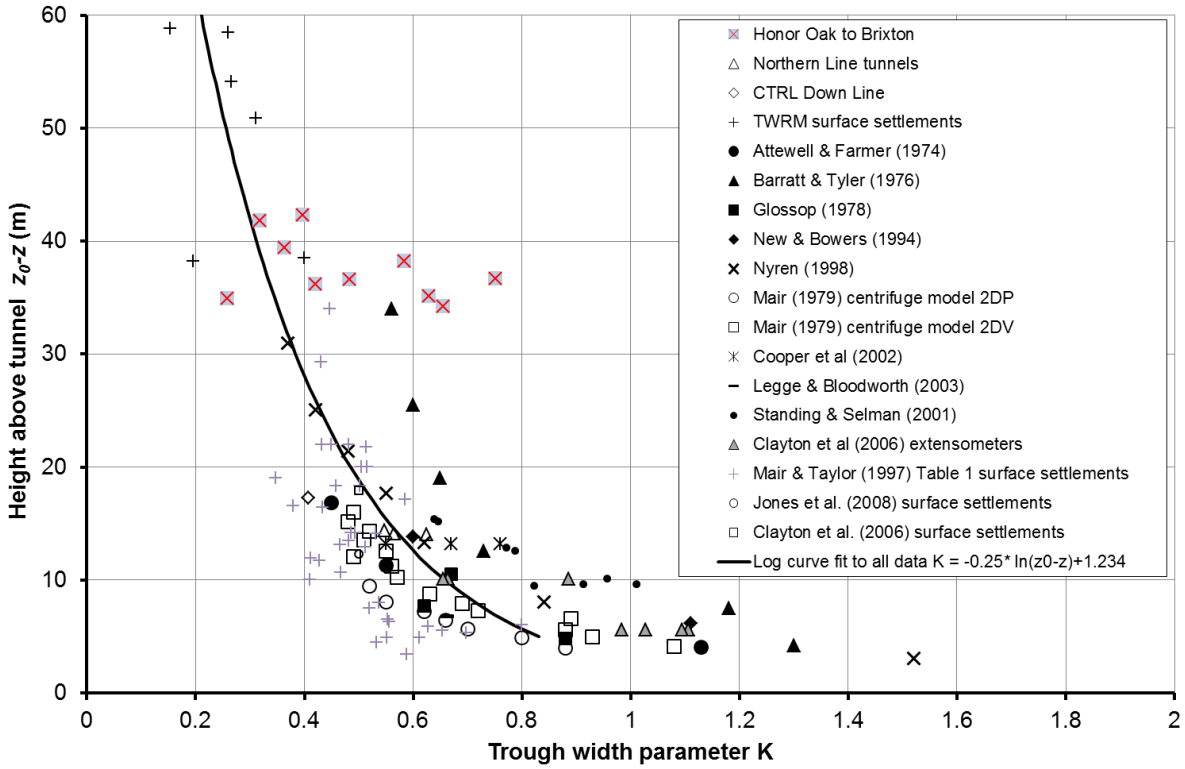

Figure 41: Trough width parameter *K* with height above the tunnel $z_o - z$ for surface and subsurface settlement profiles above tunnels in clays

The Brixton to Honor Oak data show a large variation in trough width, and perhaps wider trough widths than expected. This may have been due in part to the configuration of the settlement monitoring arrays. The Monte Carlo analysis in Chapter 2 demonstrated that standard deviation of trough width was higher at low error ratios for Array type A, which was a similar array configuration to the ones used for Honor Oak to Brixton, in that it had only 5 monitoring points.

Rather than supporting the Stoke Newington to New River Head work, the Honor Oak to Brixton data muddies the waters. However, with such a variability in results, as illustrated in Figure 41, it is difficult to draw any conclusions and so the situation remains unchanged.

The mean and standard deviation of the Honor Oak to Brixton trough width parameter values is compared to the Stoke Newington to River Head values in Table 8. As well as the trough width parameter values being generally larger, the standard deviation of the Honor Oak to Brixton trough width parameter values is nearly twice as large as for the Stoke Newington to New River Head tunnel.

	No. of trough width parameter values	Min	Mean	Max	Standard deviation
Honor Oak to Brixton	10	0.258	0.486	0.752	0.162
Stoke Newington to New River Head	6	0.153	0.264	0.400	0.087

Table 8: Comparison of calculated trough width parameter values for Honor Oak to Brixton and Stoke Newington to New River Head tunnels

6 CONCLUSIONS

Monte Carlo analysis is the only way in which the difference between various Gaussian curve-fitting methods could be compared in a rational, repeatable and quantifiable manner.

The Monte Carlo analyses presented in Chapter 2 provide valuable insight to the reliability of Gaussian curve fitting methods for different values of error ratio, trough width and for different settlement monitoring array configurations.

The Monte Carlo analyses showed that a nonlinear regression analysis (NRSAE) is the most reliable method of Gaussian curve-fitting. Although the most reliable method of calculating trough volume was by trapezoidal integration (DC), nonlinear regression provides a best fit to both trough volume and trough width. As error ratio increases and the measurement errors become negligible relative to the magnitudes of the settlements, the reliability of all curve-fitting methods improves.

When using the nonlinear regression method on real data, the standard deviation of the trough width can be estimated based on Figures 5 to 10, and the standard deviation of trough volume can be estimated based on Figures 15 to 17.

For most practical purposes, the lowest error ratio to achieve acceptable estimates of Gaussian curve parameters is between 4 and 8. This corresponds to a maximum settlement of between 1 and 2 mm used with a monitoring method with a standard deviation of measurement error of 0.25 mm. This would roughly correspond to precise levelling with a repeatability of ± 0.5 mm with maximum settlements greater than 1 to 2 mm (depending on the configuration of the array and the trough width).

Accuracy may be improved by using arrays with more points. In particular, use of a settlement monitoring array with a configuration similar to array type A is not recommended, as multiple minima may occur in the nonlinear regression analysis, which makes convergence to a solution difficult. That being said, there was little difference in reliability between array types B and C.

It was hoped that the Honor Oak to Brixton surface settlement data would provide additional information about settlement trough width at depths greater than 35m. Unfortunately, due to the generally wider trough widths found on this project, the hypothesis that trough widths for deep tunnels may be underestimated by established methods was not corroborated. However, due to the poor repeatability of the trough width parameter values, neither could it be said that the hypothesis was disproven, particularly given the evidence supporting the reliability of the Stoke Newington to New River Head measurements. More, careful, research is required to establish the truth beyond doubt.

REFERENCES

Attewell, P. B. & Farmer, I. W. (1974). Ground deformations resulting from shield tunnelling in London Clay. *Can. Geotech. J.* **11**, 380-395.

Barratt, D. A. & Tyler, R. G. (1976). *Measurements of ground movement and lining behaviour on the London Underground at Regent's Park*. Laboratory Report 684. Crowthorne: Transport and Road Research Laboratory.

Clayton, C. R. I., van der Berg, J. P. & Thomas, A. H. (2006). Monitoring and displacements at Heathrow Express Terminal 4 station tunnels. *Géotechnique* **56**, No.5, 323-334.

Cooper, M. L., Chapman, D. N., Rogers, C. D. F. & Chan, A. H. C. (2002). Movements of the Piccadilly Line tunnels due to the Heathrow Express construction. *Géotechnique* **52**, No.4, 243-257.

Glossop, N. H. (1978). *Soil deformation caused by soft ground tunnelling*. PhD thesis, University of Durham.

Jones, B. D. (2010). Low-volume-loss tunnelling for London Ring Main Extension. *Proc. Instn. Civ. Engrs. Geotechnical Engineering* **163**, June, Issue GE3, 167-185.

Jones, B. D., Thomas, A. H., Hsu, Y. S. & Hilar, M. (2008). Evaluation of innovative sprayed-concrete-lined tunnelling. *Proc. Instn Civ. Engrs Geotechnical Engineering* **161**, June, Issue GE3, 137-149.

Lake, L. M., Rankin, W. J. & Hawley, J. (1996). *Prediction and effects of ground movements caused by tunnelling in soft ground in urban areas*, CIRIA Project Report 30, 130pp. London: CIRIA.

Legge, N. B. & Bloodworth, A. G. (2003). Surface and subsurface structural response on the City of London Cable Tunnels project. *Building Response to Tunnelling: Conference Proceedings*, CIRIA Special Publication 201, pp.349-358. London: CIRIA.

Leica Geosystems (last accessed 17/7/09). *Leica DNA03/DNA10 User Manual version 2.0 English*, http://www.speedyhire.com/uploads/pdfs/survey/Leica_DNA_10_user_manual.pdf, 158pp.

Mair, R. J. (1979). *Centrifugal modelling of tunnel construction in soft clay*. PhD thesis, University of Cambridge.

Mair, R. J. & Taylor, R. N. (1997). Bored tunnelling in the urban environment. Theme Lecture, Plenary Session 4. *Proc. 14th Int. Conf. Soil Mechanics and Foundation Engineering*, Hamburg, Vol.4, pp.2353-2385.

Mair, R. J., Taylor, R. N. & Bracegirdle, A. (1993). Subsurface settlement profiles above tunnels in clay. *Géotechnique* **43**, No.2, 315-320.

New, B. M. & Bowers, K. H. (1994). Ground movement model validation at the Heathrow Express trial tunnel. *Tunnelling '94, Proc. 7th Int. Symp. IMM and BTS*, London, UK, 310-329. London: Chapman and Hall.

Nyren, R. J. (1998). *Field measurements above twin tunnels in London Clay*. PhD thesis, Imperial College, University of London.

O'Reilly, M. P. & New, B. M. (1982). Settlements above tunnels in the United Kingdom: their magnitude and prediction. *Proc. Tunnelling '82*, pp.173-181. London: IMM.

Peck, R. B. (1969). Deep excavations and tunnelling in soft ground. *Proc. 7th Int. Conf. Soil Mechanics and Foundation Engineering*, Mexico City, State of the Art Volume, 225-290.

Schmidt, B. (1969). *Settlements and ground movements associated with tunnelling in soils*. PhD Thesis, University of Illinois, Urbana.

Standing, J. R. & Selman, R. (2001). The response to tunnelling of existing tunnels at Waterloo and Westminster. *Building Response to Tunnelling*, CIRIA Special Publication 200, pp.509-546. London: Thomas Telford.

Van der Berg, J. P., Clayton, C. R. I. & Powell, D. B. (2003). Displacements ahead of an advancing NATM tunnel in the London Clay. *Géotechnique* **53**, No.9, 767-784.